Towards a human *in* vitro model of Idiopathic Pulmonary Fibrosis: Determining the effects of stiffness, dimensionality, and serum on healthy and diseased human lung fibroblast force generation

Avital Horowitz

Department of Chemical Engineering

McGill University, Montreal

Montreal Quebec, Canada

July 2016

A thesis submitted to McGill University in partial fulfillment of the requirements for the degree of Masters of Engineering

Abstract

Idiopathic pulmonary fibrosis (IPF) is characterized by the progressive stiffening of the lung matrix of unknown etiology. The end effector cell of IPF is the fibroblast which under pathological conditions differentiates into a significantly more contractile and synthetic myofibroblast cell type. At this point in time, there is no effective cure for IPF. Rodent IPF models do not recapitulate many key features of IPF, and there is a need for a human *in vitro* model of IPF in order to study IPF disease progression and provide a platform for drug discovery. The aim of this study is to uncover parameters that are often ignored in conventional *in vitro* studies that may significantly affect lung fibroblast force generation. We hypothesize that stiffness, dimensionality, and serum-supplementation of the culture system effects the biomechanical output of primary IPF and healthy lung fibroblasts. Using traction force microscopy, we studied the effects of each of these parameters in isolation and in combination to understand how the biomechanical output IPF and healthy lung fibroblasts are affected by these factors. We demonstrate that in 2D, serum supplementation greatly affects cellular traction force generation, but in 3D, cellular traction forces are unaffected by the presence of serum indicating that cells behave differently in 2D compared to 3D. Furthermore, cells increase traction forces in response to matrix stiffness in 2D (in absence of serum) and 3D demonstrating that stiffness is an important parameter that regulates fibroblast force generation *in vitro.*

Resumé

La fibrose pulmonaire idiopathique (FPI) se caractérise par une rigidification progressive de la matrice extracellulaire des poumons dont l'étiologie reste inconnue. La dernière cellule effectrice de la FPI est le fibroblaste, qui, en conditions pathologiques, se différencie en type cellulaire myoblastique significativement plus contractile et aux capacités de synthèse supérieures. Il n'y a, pour le moment, pas de traitement contre la FPI. Nombre de caractéristiques clés de la FPI ne sont pas reproduits par les modèles de rongeurs atteints de FPI et un modèle humain *in vitro* de FPI serait nécessaire en vue d'étudier la progression de la maladie FPI et de fournir une plateforme de développement de médicaments. Le but de cette étude est de déterminer les paramètres qui sont souvent ignorés lors des études *in vitro*, et qui pourraient affecter de manière significative la génération de force des fibroblastes pulmonaires. Nous avons émis l'hypothèse que la rigidité, la dimensionnalité et la supplémentation du sérum du système de culture ont un effet sur la production biomécanique finale des fibroblastes pulmonaires atteints de FPI primaire et sains. Grâce à la technique de « Traction Force Microscopy » (Microscopie de Force de Traction), nous avons étudié les effets de chacun de ces paramètres, seuls ou combinés, pour comprendre comment le rendement biomécanique des cellules FPI et NLF sont affectés par ces facteurs. Nous avons démontré que la supplémentation du sérum stimule une augmentation artificielle et robuste des forces générées par les cellules dans un système en 2D, ce qui suggère que le sérum ne fournit pas des conditions adéquates pour l'étude des caractéristiques biomécaniques des fibroblastes. De plus, une augmentation des forces de traction en réponse à la rigidité de la matrice a uniquement été décelée pour les deux types cellulaires dans le cas où ils étaient soumis à des signaux tridimensionnels, suggérant que les caractéristiques biomécaniques des fibroblastes seraient mieux étudiées dans des microenvironnements 3D.

Acknowledgements

First I would like to thank my mentor and supervisor, Dr. Chris Moraes. This thesis represents a first for the both of us, and I am extremely grateful for your insightful guidance, unconditional patience, and brilliant puns.

People, like cells, are highly responsive to their microenvironments. I would like to thank my lab mates for creating a positive lab microenvironment full of support, laughs, and good vibes. Wontae, we started out on a small lab bench together and we have been through many lab moves, cleanups, and undergrad trainings together. Thank you for your patience when answering all of my engineering-related questions. You are a diligent scientist and I am confident that you will make great strides with your PhD research and beyond. To the members of the fiesta committee, Ray, Sanya, and Stephanie thank you for boosting lab morale through the planning of fun activities that I never attend. Stephanie, you prevented many hunger-induced panic attacks and I am infinitely grateful for all the snacks.

To the members of the Leask and Hoesli Labs- Lisa, Stephanie, Natalie, Karen, Alex E, Roya, and Scott thank you for your encouragement, effective discussions, and helping me keep it somewhat together.

Outside the lab, I would like to thank my family, Mom, Dad, Chava, and Naftali for your love, support, and especially your unconditional acceptance. Mom and dad I must thank you for my curious mind, stubborn nature, and ambitious character all of which are necessary qualities of a good scientist.

I would like to thank my fiends Alex CK, Leiba, Aviya, Emeric, Miklós, Dustin, Matt, Daryan, Dan, and Jordan. Thank you Jeanne for translating my abstract into French. You are all incredibly intelligent and driven people and I am so grateful that you are all a part of my life. They say a person is the average of those they surround themselves with, so I suppose that means I am pretty awesome.

Finally, Ira. Thank you for everything.

Contribution of Authors

The following manuscript is primarily the work of the author with contributions by Dr. Chris Moraes and Ms. Wontae Lee.

Dr. Chris Moraes conducted the collagen microgel contraction experiment and aided in the experimental design and editing of this manuscript.

Wontae Lee conducted the rheological characterization of the polyacrylamide gels.

But the Hebrew word, the word timshel- 'thou mayest''- that gives a choice. It might be the most important word in the world. That says the way is open. That throws it right back on a man. For if 'Thou mayest' – it is also true that 'Thou mayest not'.

- *John Steinbeck, East of Eden*

Table of Contents

List of Figures

List of Tables

Introduction

Idiopathic pulmonary fibrosis (IPF) is a chronic disease characterized by the progressive and ultimately fatal stiffening of the lung matrix of unknown etiology (Wolters, Collard, & Jones, 2014). Histologically, IPF is characterised by a honeycomb pattern with fibroblastic foci, increase in collagen, and decrease in lung epithelial cells (Figure 1)(Kim, Collard, & King, 2006; Noble, Barkauskas, & Jiang, 2012). Increase in lung stiffness not only sabotages the natural recoil of the lung, but also the excess scar tissue in the alveoli causes inefficient oxygen diffusion resulting in difficulty breathing (Young & Bye, 2011). Patients present with cough, dyspnea, and fatigue (Daccord & Maher, 2016). IPF is the most common interstitial pneumonia, and has a poor prognosis of 2-4 years after diagnosis (Renzoni, Srihari, & Sestini, 2014).

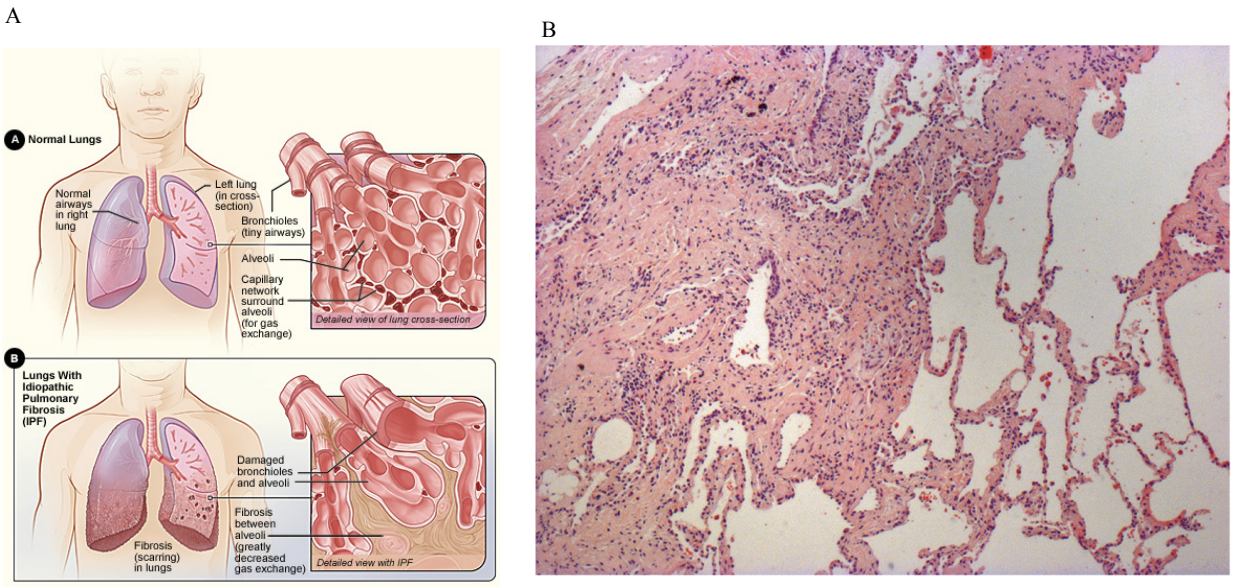

Figure 1. Idiopathic Pulmonary Fibrosis. A) Schematic of healthy lung compared to lungs affected with IPF. National Heart Lung and Blood Institute (NIH, Public Domain). B) Histological sample of characteristic fibroblastic foci in alveolar septa in 63-year-old male diagnosed with IPF. Reused with permission from (Daccord & Maher, 2016).

The effector cell of fibrosis is the fibroblast, which under pathological conditions differentiates into a more synthetic and contractile cell type called the myofibroblast (Figure 2)

(Bochaton-Piallat, Gabbiani, & Hinz, 2016). Myofibroblasts are functionally and biochemically distinct from fibroblasts, they express α-smooth muscle actin (α-SMA), organized stress fibre arrays, and increased collagen I synthesis (Tomasek, Gabbiani, Hinz, Chaponnier, & Brown, 2002). They are normally found surrounding ducts, uterine tissue, and an important component of the wound healing pathway (Hinz et al., 2007). Understanding of the pathogenesis of IPF has shifted away from chronic inflammation and towards a model of dysregulated wound healing in response to chronic alveolar epithelial micro injury (Selman, King, & Pardo, 2001).

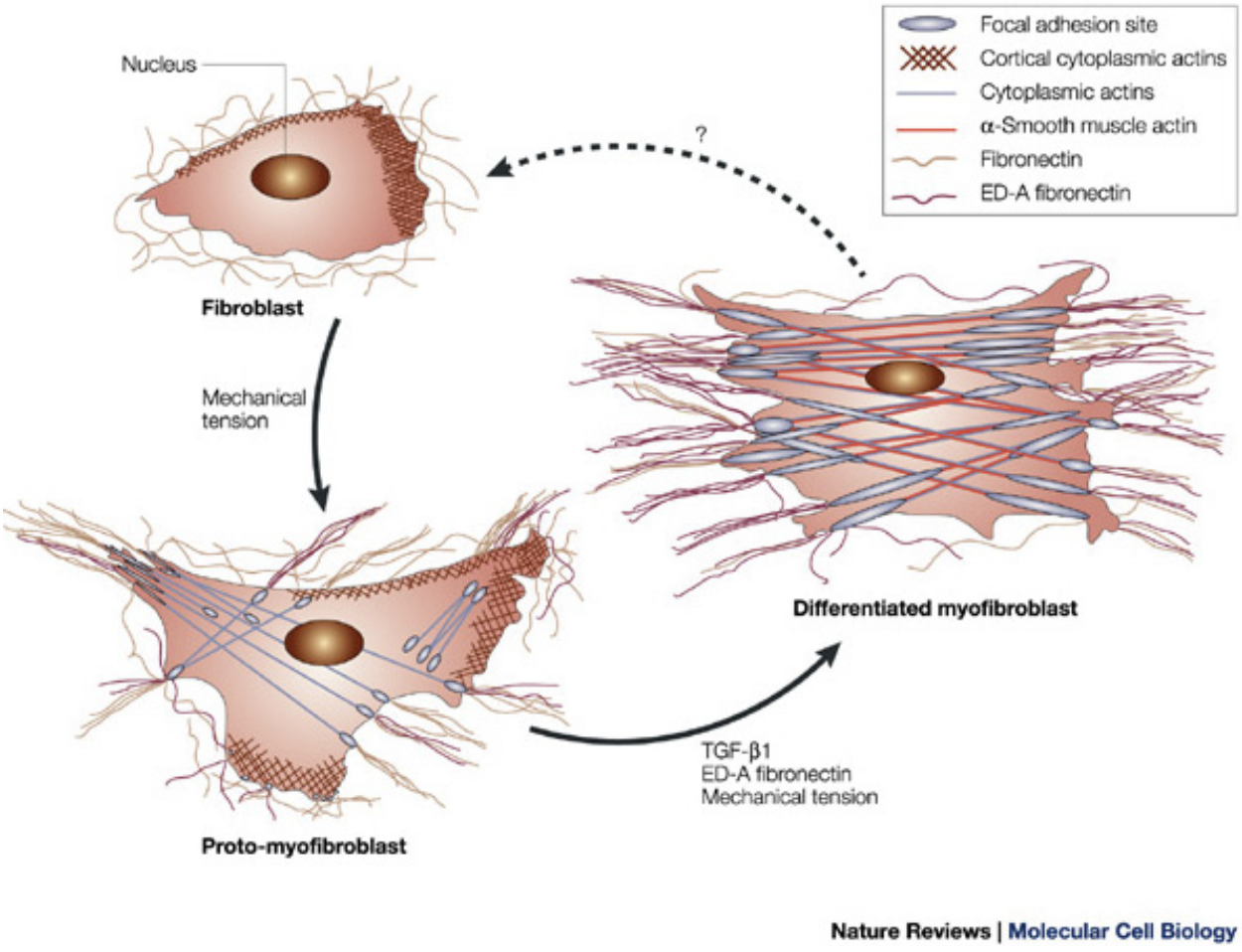

Figure 2. Fibroblast differentiation into myofibroblasts. Upon increase in mechanical tension and soluble factors including TGF-β and fibronectin, fibroblasts differentiate into myofibroblasts. Myofibroblasts are biochemically distinct from fibroblasts and display *de novo* α-SMA incorporation into actin stress fibres. Proto-myofibroblasts are an intermediary cell type that expresses a stress fibre array but do not express α-SMA. Reused with permissions from (Tomasek et al., 2002)

The accepted mechanism underlying the pathogenesis of IPF, is a prolonged and unregulated fibroproliferative repair response. Under normal wound healing conditions, fibrosis is the process wherein myofibroblasts synthesize extracellular matrix (ECM) to replenish matrix lost during wounding, and contract in order to bring wound borders together with the purpose of re-establishing the integrity of the damaged tissue (Bochaton-Piallat et al., 2016). When normal wound healing is complete, the myofibroblasts are removed either by apoptosis or de-differentiation back into fibroblasts (Tomasek et al., 2002). During abnormal wound healing, as seen in fibrotic diseases, these myofibroblasts persist and continue to synthesize ECM and contract in an unregulated manner (Klingberg, Hinz, & White, 2013).

At this point in time, there is no cure for IPF. Of the many compounds that have shown to be antifibrotic in mouse models, only a small fraction has been proven promising in human clinical trials (Moeller, Ask, Warburton, Gauldie, & Kolb, 2008). Two compounds Nintedanib and Prifendone have recently been US FDA-approved for the treatment of IPF, and although they have been shown to inhibit fibrosis progression, their ability to effectively decrease IPF-related mortality is unclear (Canestaro, Forrester, Raghu, Ho, & Devine, 2016). No compound has ever been shown to be as effective in humans as in mouse models (Moeller et al., 2008). Currently, the bona fide model of IPF is the bleomycin rodent model. Bleomycin is chemotherapeutic drug that induces pulmonary fibrosis by initiating an acute lung injury and inflammatory response. The rodent bleomycin model has the benefits of an animal model in that it is relatively easy, fast and reproducible (Reinert, #xe1, Baldotto, Nunes, & Scheliga, 2013). While it has helped uncover key molecular mechanism and biochemical players important in IPF disease (Zhao et al., 2002), its use as a drug discovery platform is questionable. This is because the model does not accurately capture the human disease for a number of reasons mainly, the

speed of onset and the reversibility of bleomycin-induced fibrosis do not recapitulate the chronic and irreversible nature of IPF (Izbicki, Segel, Christensen, Conner, & Breuer, 2002). This results in the development of drugs that do not pass human clinical trials, representing time and financial investments of 10-12 years and 2.5 billion dollars on average (DiMasi, Grabowski, & Hansen, 2016).

There is a need for a human *in vitro* model of IPF in order to provide an authentic platform to study IPF disease and discovery drugs or therapies. Organ-on-a-chip technologies have made great strides developing physiologically-realistic *in vitro* systems for many organs and diseases (Ingber, 2016). However, these technologies are very organ- and disease-specific and the parameters that would be important for an IPF culture system need to be elucidated.

Recently, 3D culture systems have been shown to be more physiologically realistic than 2D stiff tissue culture plastics (B. M. Baker & Chen, 2012). Cells have been shown behave differently in 3D matrices compared to 2D cultures, including difference in spread area, morphology, and differentiation (Harunaga & Yamada, 2011; Joaquin et al., 2016; Y. Li & Kilian, 2015). In recent decades, a plethora of 3D cell culture strategies have been developed raising the question of what constitutes a 3D culture system. These methods range from 3D collagen scaffolds (Leung et al., 2015; Moraes, Simon, Putnam, & Takayama, 2013), narrow microchannels (Stroka et al., 2014), and sandwich culture systems whereby cells are enclosed between two hydrogels (Ballester-Beltrán, Moratal, Lebourg, & Salmerón-Sánchez, 2014; Ballester-Beltrán, Lebourg, & Salmerón-Sánchez, 2013; Beningo, Dembo, & Wang, 2004). Although these different methods evoke a wide-range of cellular behaviours, they demonstrate that dimensionality in cell culture determines important cellular behaviours. Most *in vitro* IPF studies have been done using fibroblasts cultured on 2D planar substrates (Marinković, Liu, &

Tschumperlin, 2013; Prasad, Hogaboam, & Jarai, 2014) and therefore fibroblast behaviour may be compromised and not capture how the disease progresses *in vivo*. Therefore, it is important to elucidate the effects of dimensionality on lung fibroblast biomechanics *in vitro*.

In addition to the dimensionality of the culture system, other physical properties, such as matrix stiffness has been recently shown to alter cell behaviour (Wesley R. Legant et al., 2010). Tissues in the body are heterogeneously stiff ranging several orders of magnitude (Figure 3). Matrix stiffness has been shown to guide spread area, migration, traction forces, and lineage-specification of naïve stem cell (Engler, Sen, Sweeney, & Discher, 2006; Yeung et al., 2005). The elastic modulus (E) of healthy lung tissue is 1 kPa in stiffness, and stiffens up to 20 kPa in IPF disease (Liu et al., 2010). Probing cellular forces *in* vitro has demonstrated that matrix stiffness plays a crucial role in myofibroblast differentiation and IPF disease progression *in vivo*, and therefore an important parameter to integrate in an *in vitro* study of IPF and NLF fibroblast biomechanical output (Marinković et al., 2013).

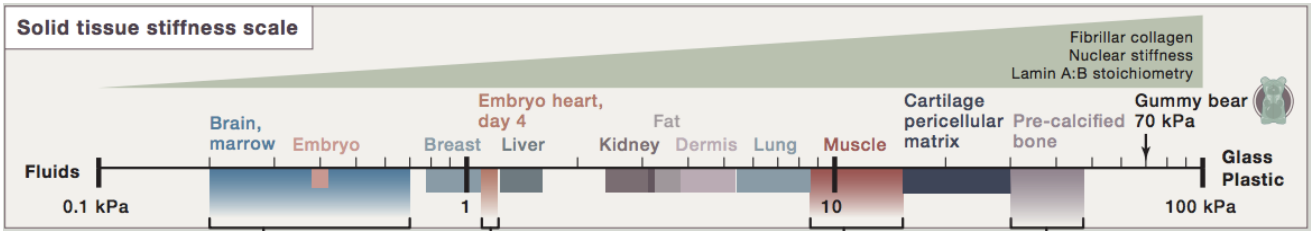

Figure 3. Range of tissue stiffness. Tissues stiffness ranges several orders of magnitude, Ranging from > 1 Pa for neural tissue to GPa for calcified bone. Healthy lung stiffness is around 1 kPa. Reused with permission from (Irianto, Pfeifer, Xia, & Discher, 2016)

Furthermore, fetal bovine serum (FBS) is the gold-standard supplement added to universally all cell culture media that allows cells to proliferate and survive *in vitro*. The contents of FBS are largely undefined, and FBS has been shown in many instances to alter cell behaviour and phenotype (Gillery, Maquart, & Borel, 1986). FBS has been linked to the activation of

specific target signalling pathways that promote the expression of myofibroblast-like genes (Small, 2012). Unpublished collagen contraction data that utilizes an aqueous two-phase system to create fibroblast-containing collagen microgels (Figure 4), indicated that a significant difference in collagen contraction between normal lung fibroblasts (NLF) and IPF fibroblasts was only seen in conditions of serum-starvation. This suggests that serum does in fact stimulate an artificial contraction in normal fibroblasts, demonstrating that FBS may not provide an accurate backdrop to quantify IPF biomechanics *in vitro*.

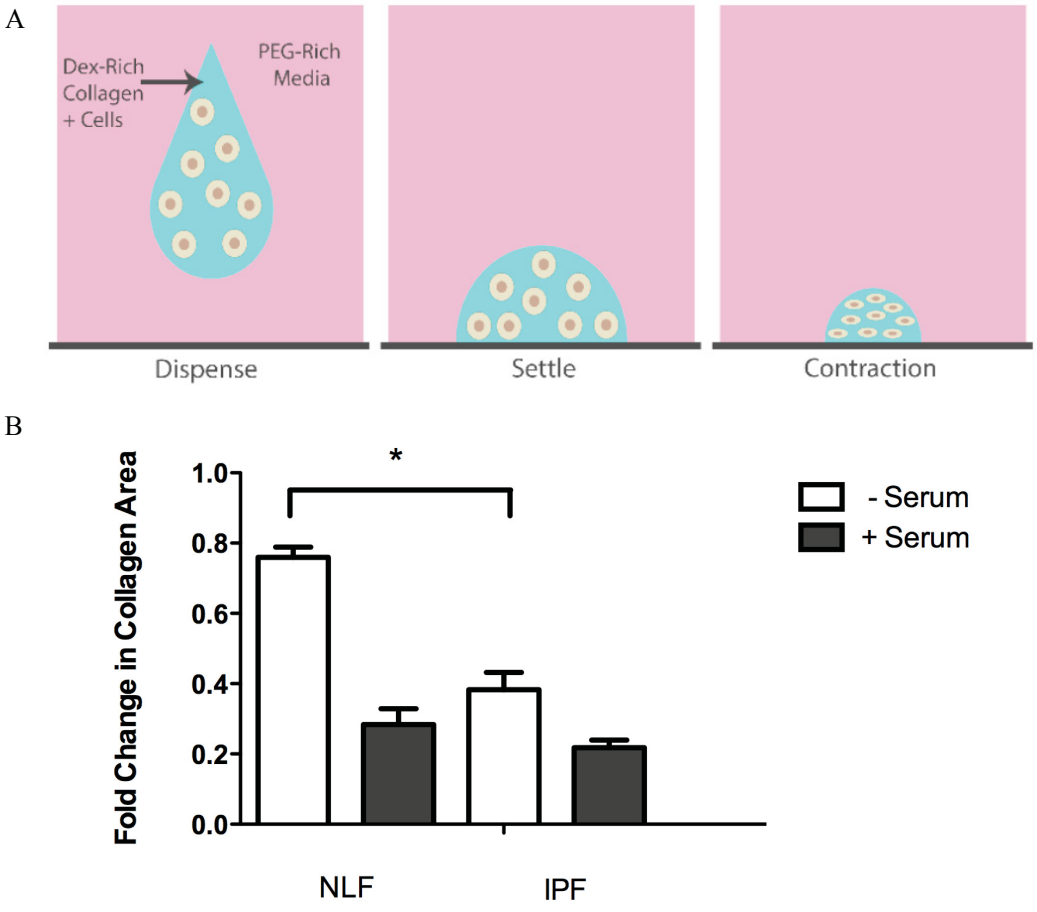

Figure 4. Serum stimulates robust and artificial contraction in primary lung fibroblasts. A) Collagen microgels were made using an aqueous two phase system whereby a dextran/collagen/cells droplet phase separated from surrounding PEG-rich media. The droplet was then allowed to settle and cell contraction was measured by optical observation of decrease in collagen gel size resulting from cellular contraction. B) Significant difference in IPF and NLF contraction was only seen in conditions of serum-starvation. One-way ANOVA, SNK post-test, *= $P<0.05$, n=3-6.

IPF is essentially a disease of aberrant cellular contraction and tissue remodelling (Renzoni et al., 2014). Therefore, determining the functional output of cells such as, traction forces which are closely related to tissue remodelling, in response to various factors will provide tremendous insight as to which parameters are important for a model of IPF. In sum, there is a need for an *in vitro* model of human IPF, and an understanding of which parameters are important for recapitulating a human IPF culture system.

Hypothesis and Research objectives

The goal of this research is to understand the parameters that are important for quantifying IPF biomechanics *in vitro*. We hypothesize that dimensionality and stiffness of the culture system and serum supplementation will affect healthy and diseased lung fibroblasts biomechanical output.

i) Determine the effects of serum and matrix stiffness on IPF and NLF traction forces using conventional traction force microscopy

ii) Study the effects serum and matrix stiffness on IPF and NLF traction forces and morphology using 3D traction force microscopy to determine the effects of dimensionality on these parameters.

Literature Review

Cell-Matrix Interactions

The ECM is a dynamic and acellular component of tissues that is comprised of a combination of polysaccharides, growth factors, and proteins including collagen, fibronectin, laminin, and elastin (Y. Li & Kilian, 2015). Cells constantly degrade, synthesize, and remodel their surrounding ECM in both healthy and diseased states (Cox & Erler, 2011), and fibroblasts are the main cells that build and maintain the ECM in most soft connective tissue. Both the biochemical and physical properties of the ECM have been shown to control many cellular processes, and it is this interplay between mechanical properties and matrix composition that will dictate a wide range of specific cellular responses. For instance, the ECM serves as a storage for soluble factors that regulate cellular functions (Bonnans, Chou, & Werb, 2014). These soluble factors can be released through many mechanisms including proteolytic degradation of the ECM by cell-secreted proteases, or by mechanical tugging of cells. This illustrates not only a means by which cells can control the spatio-temporal release of ECM-bound factors, but another means in which mechanical and biochemical signalling are interconnected (B. M. Baker & Chen, 2012). The importance of the proper mechanical and biochemical ECM properties is evident since an aberrant ECM underlies many diseases including cancer and fibrosis.

The stiffness of the ECM has been shown to be an important mechanical property that regulates cell behaviour. Tissues in the body are heterogeneously stiff, ranging several orders of magnitude from neural tissue (E= 0.1-1 kPa) to bone (E= GPa), and matrix stiffness has been shown to dictate many cellular processes including cell morphology, migration, and differentiation (Murphy, McDevitt, & Engler, 2014). On stiff materials, cells increase spread area, form actin stress fibres, and larger focal adhesions as compared to cells adhered to soft

materials resulting in differences in protein expression and cellular behaviour (Peyton & Putnam, 2005; Yeung et al., 2005). Stiffness has also been shown to guide cellular migration, whereby many cell types undergo directed migration up a stiffness gradient, a phenomena termed durotaxis (Joaquin et al., 2016; Vincent, Choi, Alonso-Latorre, del Alamo, & Engler, 2013). Furthermore, matrix stiffness has been shown to dictate stem cell differentiation, whereby naïve mesenchymal stem cells differentiate into neural cells on soft matrices, muscle cells on intermediate matrix stiffness, and bone cells on rigid substrates (Engler et al., 2006). However, in pathological conditions such as cancer and tissue fibrosis the ECM becomes abnormally stiff leading to dysregulated cellular behaviour (Bonnans et al., 2014).

Cells sense the physical properties of the surrounding ECM via complex mechanotransduction pathways. Integrins are the main cellular component that directly connect cells to the ECM and, transmits signals from outside to inside the cell and vice versa (Humphrey, Dufresne, & Schwartz, 2014). Integrins link ECM proteins to the accompanying cytoskeletal proteins and signalling proteins of focal adhesions. Matrix stiffness information is imparted via integrins to the Rho-family of GTPases and their downstream effectors, including Rho-associated protein kinase (ROCK), which are important regulators of actin cytoskeleton and focal adhesion dynamics (Hoon, Tan, & Koh, 2016). Changes in matrix stiffness have been shown to alter actin cytoskeletal configuration, whereby increase matrix stiffness stimulates the formation of stress fibres and focal adhesions, resulting in changes in cellular behaviour (X. Huang et al., 2012). Mechanical information is transduced to the nucleus via YAP and TAZ proteins of the Hippo pathway which have been shown to contribute to stiffness-induced expression of specific genes (Dupont et al., 2011).

Myofibroblasts

Modified fibroblasts with smooth muscle-like features, myofibroblasts, were first described in granulation tissue of healing wounds (Gabbiani, Le Lous, Bailey, Bazin, & Delaunay, 1976). Myofibroblasts are more contractile and synthetic than fibroblasts, and these features allow for their key role in wound healing. During normal wound healing, fibroblasts become activated and differentiate into myofibroblasts, which generate large contractile forces and actively produce ECM proteins resulting in wound closure and remodelling of the tissue (B. Li & Wang, 2011). After wound healing is complete, these myofibroblasts are removed by apoptosis or de-differentiation back into fibroblasts. However, in pathological conditions such as fibrosis, these myofibroblasts persist and the sustained production of ECM components, including collagen, and increased contractility leading to the stiffening and disruption of the tissue architecture and function (S. K. Huang & Horowitz, 2014).

Myofibroblasts are the effector cells of tissue fibrosis, which is characterised by the aberrant accumulation and activation of myofibroblasts contributing to the stiff collagen-rich ECM observed in fibrosis. Myofibroblasts and fibroblast are not only functionally different, they are also biochemically distinct. The high contractile activity of myofibroblasts is generated by the de-novo expression of α-SMA, and incorporation into stress fibres which along with increased collagen I expression and secretion, are the hallmarks of myofibroblast differentiation (Tomasek et al., 2002). Myofibroblast phenotype is regulated primarily by transforming growth factor β (TGF- β), and increase matrix mechanical stiffness, and the ED-A domain of fibronectin (Serini et al., 1998). Interestingly, not all myofibroblasts express α-SMA and are referred to as proto-myofibroblasts. Protomyofibroblasts are an intermediary cell type between fibroblasts and protomyofibroblasts that have organized stress fibre arrays but do not express α-SMA, and they

are found in several location *in vivo* including the alveolar septa. While myofibroblast and fibroblasts are easily distinguished from protomyofibroblats *in vivo*, when cultured on hard tissue culture plastic in the presence of FBS, virtually all fibroblasts acquire proto-myofibroblastic phenotype (Tomasek et al., 2002)

Myofibroblasts are functionally different from smooth muscle cells as well. Contractile differences between myofibroblasts and smooth muscle cells underlies the remodelling behaviour of myofibroblasts. Smooth muscle cell contraction is rapid and short in duration whereas myofibroblasts contraction is slow and long-lasting resulting in the chronic remodelling of the tissue (Bochaton-Piallat et al., 2016). In addition to conventional smooth muscle contraction mechanisms, myofibroblast contractile activity is also regulated by the Rho/ROCK/myosin light chain pathway imparting functional differences between smooth muscle cells and myofibroblasts (Tomasek et al., 2006).

During fibrosis, local fibroblasts are a major source of myofibroblastic cells. However, myofibroblasts may develop from other resident cellular precursors including smooth muscle cells in atherosclerosis, and transdifferentiation of alveolar epithelial cells in pulmonary fibrosis (K. K. Kim et al., 2006). Myofibroblasts may also develop from circulating cells such as bone marrow-derived fibrocytes and mesenchymal stem cells (Xu et al., 2015).

Idiopathic Pulmonary Fibrosis

Idiopathic pulmonary fibrosis (IPF) is a devastating and progressive fibrosing disease with no known cause or cure. IPF is the most common form of interstitial lung disease that effects an estimated 50 in 100,000 people (Raghu, Weycker, Edelsberg, Bradford, & Oster, 2006), and poor prognosis with a median survival of 3 years after diagnosis. IPF is aging-related, and is diagnosed by the histological pattern of usual interstitial pneumonia with no known

underlying cause. Histologically, IPF is characterized by the remodelling of the lung architecture with heterogeneous fibroblastic foci, honeycombing, increase in collagen, and loss of alveolar epithelial cells (D. S. Kim et al., 2006). The effector cell in IPF is the fibroblast which under pathological conditions differentiates into myofibroblast which is significantly more contractile and synthetic than normal fibroblasts resulting in the formation of scar tissue in the lung pleura (S. K. Huang & Horowitz, 2014). Increase in alveolar scar tissue not only disrupts the natural elasticity of the lung that is required for breathing, it also increases the diffusional area of oxygen, significantly impairing efficient oxygen exchange (Young & Bye, 2011).

Although biochemical factors have traditionally been attributed to IPF disease initiation and progression, it has become recently apparent that matrix and cell biomechanics plays a crucial role if IPF initiation and progression. In the most severe cases of IPF, the stiff matrix and aberrant myofibroblast engage in a perpetuating positive feedback loop, whereby matrix stiffness stimulates myofibroblasts activation and subsequently more matrix synthesis and contracting resulting in increased matrix stiffness (Liu et al., 2010). This can be partially elucidated by activation mechanism of the potent fibrosis and myofibroblast regulator, TGF-β (Roberts et al., 1986). TGF-β is kept in an inactive form entrapped within the ECM, and is released and activated upon mechanical tugging by surrounding myofibroblasts (Wipff, Rifkin, Meister, & Hinz, 2007). The release TGF-β from its latent complex by tension produced by myofibroblast contraction on matrices of pathological stiffnesses, furthers the self-perpetuating state of IPF(Liu et al., 2010). However, to what extent IPF is caused by a diseased matrix that alters otherwise normal cells, or intrinsically aberrant cells that remodel a healthy matrix, or if it is a combination between the two, remains unknown. Recent evidence suggests that matrix stiffness is a potent stimulator and possible initiator of IPF (Liu et al., 2010), whereby IPF fibroblasts remained

highly responsive to changes in matrix stiffness, and both proliferative and contractile differences between IPF and NLFs were attenuated on physiologically soft matrices, suggesting that fibroblast response to mechanical cues may offer unique and potent drug targets for treating IPF (Marinković et al., 2013).

The understanding of the pathogenesis of IPF has evolved from a model chronic inflammation and towards a mechanism of aberrant wound healing in response to recurrent alveolar epithelial microinjury. Under healthy conditions, once myofibroblasts have successfully remodelled the wounded ECM, they disappear via apoptosis or revert back into fibroblasts. However, myofibroblasts found in lung fibroblastic foci, persists and evade apoptosis and continue to synthesize and contract the ECM contributing to the progressive formation of scar tissue within alveolar septa (S. K. Huang & Horowitz, 2014). Gastroesophageal reflux disease (GERD) is a co-morbidity of IPF (Tobin et al., 1998), and it has been hypothesized that chronic alveolar microinjury may be caused by microaspirations of acidic gastric contents associated with GERD (Lee et al., 2010). Exposure of alveolar epithelial cells to acidic gastric contents has been shown to create alveolar microinjuries that are strikingly similar to *in vivo* IPF (Felder, Stucki, Stucki, Geiser, & Guenat, 2014), suggesting that alveolar wounding caused by GERD may be a key initiator of IPF.

At this point in time there is no effective cure for IPF. Although there are drugs on the market aimed at treating IPF, none of them actually cure or reverse IPF, and many are accompanied by adverse side effects (Rangarajan, Locy, Luckhardt, & Thannickal, 2016). Nintedanib and Prifendone are two US Food and Drug Administration (FDA)-approved therapies for the treatment of IPF. The pharmacological mechanism of prifendone is not well-understood, but it is thought to inhibit TGF-β-induced EMT, myofibroblast activation, and collagen synthesis

(Raghu, Johnson, Lockhart, & Mageto, 1999) . Similarly, nintedanib, a tyrosine kinase inhibitor, inhibits cytokines that are known to stimulate fibroblast proliferation and myofibroblast differentiation (Wollin et al., 2015). A recent comprehensive review of all IPF-targeted therapies demonstrated that although pirfenidone and nintedanib slow the rate of IPF progression, they have not been shown to effectively decrease respiratory-induced mortality (Canestaro et al., 2016).

Current Models of IPF

Various animal models been developed to investigate potential therapies for IPF. Common methods to induce fibrosis in animals, include radiation damage, inhalation of bleomycin, silica or asbestos, or transgenic mice models employing fibrotic cytokine (Moeller et al., 2008). The most common is the bleomycin model in mice and rats. Bleomycin is a chemotherapeutic antibiotic, and its use as an IPF-stimulator in animal models is based on on the fact that pulmonary fibrosis is a common contraindication of bleomycin in human cancer treatment (Adamson & Bowden, 1974). Lungs are specifically susceptible to bleomycin-induced fibrosis since bleomycin hydrolase, a bleomycin inhibiting enzyme that critically influences the effectiveness of this drug, is found in very low concentrations in the lungs (Reinert et al., 2013).

The bleomycin rodent model has many advantages in that fibrosis-induction is relatively fast, easy, and most critically, reproducible. This model has helped elucidate many key molecular compounds and cytokines important for IPF, such as the *in vivo* mechanism of TGF-β activation (Zhao et al., 2002). However, despite its usefulness, the bleomycin model has significant limitations in reproducing the progressive, chronic, and irreversible nature of IPF. Aside from inherent differences between human and rodent airway physiology (Wright, Cosio, & Churg, 2008), in the bleomycin model, the fibrosis evolves over weeks, whereas in IPF, the

fibrosis evolves over years (Moeller et al., 2008). Furthermore, bleomycin-induced fibrosis has been shown to be reversible without any sort of intervention, which is certainly not the case for patients suffering from IPF (Izbicki et al., 2002). Currently, there is no animal model that reliably recapitulates the critical hallmarks of IPF.

Over the years many compounds have been shown to inhibit the progression fibrosis in the bleomycin rodent model. However, to date not one of these compounds has shown a comparable antifibrotic effect in human clinical trials (Moeller et al., 2008). Although the bleomycin model has aided in discovering molecular pathways important for IPF, its use as a drug discovery platform is limited. The optimal experimental model for IPF remains elusive.

Cells in Three-Dimensions

The culture of mammalian cells has conventionally been done on planar and rigid tissue culture plastic with media cocktails designed to optimize cell growth survival and proliferation *in vitro.* Recently it has become increasingly apparent that cells behave differently in three dimensional (3D) microenvironments (B. M. Baker & Chen, 2012; Kojima, Moraes, Cavnar, Luker, & Takayama, 2015; Moraes et al., 2013). Most cells naturally interact with a complex and information-rich 3D matrix, and it has become increasingly clear that biological behaviours determined from 2D studies to not necessarily translate to 3D microenvironments (Y. Li & Kilian, 2015). Most strikingly, cell morphologies alter drastically in a dimension-dependent manner, and morphology and spread area are important regulators or cell function and viability (Chen, Alonso, Ostuni, Whitesides, & Ingber, 2003). This is partially attributed to the fact that 2D planar systems inherently force an apical-basal polarity to cells, which is unnatural for mesenchymal-type cells such as fibroblasts(B. M. Baker & Chen, 2012). On 2D surfaces, fibroblasts assume a flat morphology, whereas in 3D, they adopt a unique morphologies such as

stellate or bipolar depending on stiffness and configuration of the 3D matrix (Brendon M. Baker et al., 2015; Beningo et al., 2004; Rhee, 2009). In addition to changes in cell morphology, cell adhesion dynamics are distinct in 2D compared to 3D environments, and cell adhesion play a pivotal role in cellular behaviours including migration and survival (Hakkinen, Harunaga, Doyle, & Yamada, 2011). Cells utilize integrin-based adhesions in 3D as compared to focal adhesion complexes that are mainly seen in 2D (Hakkinen et al., 2011). These inherent differences in basic cellular functions, underlie the difficulty in translating 2D studies to 3D, and why much effort has been placed on developing physiologically-relevant 3D culture systems.

With the end goal of designing culture systems that provides 3D cues to study cells *in vitro*, a plethora of strategies have been developed in the last decade resulting in a wide-range of interpretations of what constitutes a 3D system. Perhaps the most physiological are cells embedded within fibrous collagen scaffolds since collagen fibrils primarily regulate and define most tissues (Cen, Liu, Cui, Zhang, & Cao, 2008; Kojima et al., 2015; Leung et al., 2015; Moraes et al., 2013). Collagen scaffolds can be implemented to study a wide-range of biological questions including osteogenesis (Adamson & Bowden, 1974), cancer cell migration (Charras & Sahai, 2014), and fibroblast force generation (Moraes, Labuz, Shao, Fu, & Takayama, 2015).

Despite the physiological relevance of collagen scaffolds, these systems have several limitations, specifically with 3D traction force measurements. Cellular traction forces mediate many integral cellular processes including tissue homeostasis, migration, differentiation, and in many cases aberrant cellular traction forces underlies many disease pathologies (Rape, Guo, & Wang, 2011; Style et al., 2014; Tomasek et al., 2006). Understanding how these traction forces are regulated in 3D remains a fundamental question in the field and current collagen scaffold systems are limited in this application. Namely, the stiffness of collagen cannot be controlled,

the systems are complex and introduce a broad range of variables and it is difficult to unravel the origin of dimensionality (Ballester-Beltrán et al., 2014), and determining cellular force generation in 3D systems requires complex computer simulations and modeling (Wesley R. Legant et al., 2010; Toyjanova et al., 2014). In order to address these limitations, a fast and relatively simple "sandwich" strategy of introducing 3D cues to cells was developed (Beningo et al., 2004). In this approach, cells are sandwiched between two polyacrylamide gels, and this method has shown that by the introduction of dorsal adhesion, myoblasts experience enhanced differentiation (Ballester-Beltrán et al., 2013) and fibroblasts develop a more *in vivo*-like spindle morphology (Beningo et al., 2004) as compared to cells plated on 2D gels. This system is stiffness tunable and allows for straightforward calculations of 3D cellular traction force measurements.

Methods of Measuring Cellular Forces *in vitro*

Probing cellular forces *in vitro* has elucidated many key cellular behaviours involved in fibrosis progression, cancer and development. Several techniques have been developed to measure cellular forces *in vitro* (W. R. Legant et al., 2010). The simplest method for indirectly measuring cellular traction forces is through observation of cell-populated collagen gel contraction (Bell, Ivarsson, & Merrill, 1979). Fibroblasts and myofibroblasts embedded within 3D collagen matrices adopt *in vivo*-like cell shape morphologies which likely impart a physiologically-realistic contractile forces (Kanta, 2015). Depending on which confirmation is best suited to address the biological question at hand, collagen gel contraction assays can be free-floating or tethered whereby external stress is present (Ali, Chuang, & Saif, 2014). Although collagen gel contraction is a relatively fast and easy method to measure microtissue contraction and has aided in the understanding of fibroblasts biomechanics and wound healing, the technique

is insensitive to small traction forces, and instability in collagen lattice structure only gives a broad picture of cellular dynamics (Kanta, 2015; B. Li & Wang, 2011).

Traction force microscopy (TFM) is a technique that has allowed the direct calculation of traction forces exerted by single cells and confluent cell sheets in both 2D and 3D (Style et al., 2014). Cells exert traction forces via their cytoskeleton in order to mechanically attach to neighbouring cells and underlying ECM. In order to measure these traction forces, cells are adhered to linearly elastic substrates, typically polyacrylamide gels that contain fluorescent microspheres. When cells adhere to the substrate, their traction forces deform the underlying substrate imparting a specific pattern in the embedded beads. When the cell and its traction forces removed by the addition of a killing agent, the substrate returns to its references state thereby causing a displacement in the underlying beads. Calculating the displacement of the beads, similar to Hook's law, and other physical properties of the gel including Young's modulus and Poisson's ratio, provide accurate traction force measurements (Tseng et al., 2012). TFM has been instrumental in understanding traction forces exerted during cellular migration (Dembo & Wang, 1999), wound healing (Vedula et al., 2015), and tumor metastasis (Kraning-Rush, Califano, & Reinhart-King, 2012). TFM is a versatile in that it can be used in combination with other patterning techniques. For instance, polyacrylamide gels patterned with adhesive proteins demonstrated that traction forces are determined by distance of cell center to perimeter and not primarily to cell spread area (Rape et al., 2011).

Materials and Methods

Glass Coverslip and Microscope Slide Surface Modification

Glass coverslips (12 and 18 mm, diameter, Fischer Scientific, Waltham, MA) were chemically modified to allow covalent attachment of polyacrylamide gels. Briefly, the coverslips were treated with 0.4% (v/v) solution of 3-(trimethyoxysilyl) propyl methacrylate (MPS, Sigma Aldridge, St-Louis MO) in acetone (Fischer Scientific, Waltham, MA) rotating for 5 minutes at room temperature. The coverslips were then washed with fresh acetone rotating for 5 minutes at room temperature, and then placed on a paper towel to air dry before use.

To facilitate the detachment of cast PA gels, large glass microscope slides (Fischer Scientific, Waltham MA) were treated with RainX (ITW Global Brands, Houston, TX) in order to create a hydrophobic glass slide surface.

Polyacrylamide Gel Fabrication

Polyacrylamide (PA) gels we fabricated from acrylamide (40% w/v, Bio-Rad Laboratories, Hercules, CA), and *N,N*-methylene-bis-acrylamide (BIS, 2% w/v, Bio-Rad Laboratories, Hercules, CA) stock solutions based on a previous protocol (Tse & Engler, 2010). The final concentration of acrylamide/BIS was 3%/0.085% and 7.5%/0.236% (v/v) for soft gels and stiff gels respectively (Table 1). Carboxylate-modified fluorescent beads (0.2 µm, red fluorescent 580/605, Life Technologies) at a concentration of 0.1% (v/v) of the final volume. Gelation was initiated by the addition of ammonium persulfate (Bio-Rad Laboratories, Hercules, CA) and *N-N-N-N*-tetramethylethylenediamine (Sigma Aldridge, St-Louis, MO), and volume corresponding to a 50 µm gel (12.72 µL and 8.48 µL for 18 and 12 mm coverslips respectively) was dispensed onto the hydrophobic microscope glass surface. The PA droplet was sandwiched between an MPS-treated coverslip and allowed to polymerize for 10-20 minutes. Once

polymerized, the gels were placed in 12-well plates (Fischer Scientific, Waltham, MA) and washed with phosphate buffered saline (PBS, pH 7, Sigma Aldridge, St-Louis MO) and sterilized under UV for 45-60 minutes.

Table 2. Composition of polyacrylamide gels with corresponding rheological characterization.

Young's Modulus (E)	40% Acrylamide (v/v)	2% BIS (v/v)	PBS (v/v)	TEMED (v/v)	Fluorescent Beads (v/v)	1% APS (v/v)
321 Pa	3%	0.085%	77.1%	0.15%	1%	0.1%
12.3 Pa	7.5%	0.236%	67.4%	0.15%	1%	0.1%

Collagen Functionalization

To provide a surface for cellular adhesion, polyacrylamide gels were functionalized with bovine collagen I (Fischer Scientific, Waltham, MA) using the photoactivatable bifunctional crosslinked *N*-sulfosuccinimidyl-6-[4′-azido-2′-nitrophenylamino] hexanoate (sulfo-SANPAH, ProteoChem). Gels were treated with a 0.05 mg/mL solution of Sulfo-SANPAH in PBS and placed under UV for 5 minutes until the solution turned from orange to a pale yellow color. The gels were than incubated with 0.05 mg/mL solution of bovine collagen I in PBS, overnight at 4 °C. The following day, the gels were washed three times in sterile PBS shaking at room temperature.

Rheology

To characterize the stiffness of the polyacrylamide gels, 1 mm PA gels sandwiched between two 12mm MPS-treated coverslips were fabricated. The stiffness of the polyacrylamide

gels was characterized using a strain-controlled rheometer (Anton Paar MCR 302) with parallel plate geometry (8 mm plate diameter. A strain amplitude within the linear viscoelastic range (10%) was applied over a frequency range of 0.3-300 rad/s. The storage modulus (G') and loss modulus (G") were automatically reported by the Anton Paar Rheoplus software.

Cell Culture

Primary normal lung fibroblasts (NLFs) and IPF-derived fibroblasts (IPF) were obtained from the Hogaboam lab (Cedars-Sinai Medical Institute, Los Angeles, CA). Cells were cultured in Dulbecco's modified media (DMEM, Gibco), supplemented with 1% (v/v) antibiotic antimycotic solution (Sigma Aldridge, St-Louis, MO), and 15% (v/v) fetal bovine serum (FBS, Gibco), and maintained in a humidified incubator at 37 °C and 10% CO_2. When confluence was reached, cultures were washed with PBS, cells were treated with 0.25% trypsin (Gibco) for 3 minutes at 37 °C, trypsin was neutralized by adding equal volume of DMEM, and centrifuged at 200 rpm for 5 minutes in order to pellet the cells. Cells were resuspended in DMEM and a plated in fresh T-75 flask (VWR). In traction force microscopy experiments, cells were plated on collagen-functionalized polyacrylamide gels on 18 mm coverslips at a density of 1-3 $x10^3$ cells /cm^2. P7-19 cells were used.

Immunofluorescence

Cells were fixed in 4% (w/v) paraformaldehyde (Sigma Aldridge, St-Louis, MO) in PBS for 30 minutes at room temperature, and subsequently washed three times with PBS. Samples were then permeabilized via incubation with 0.1% (v/v) triton X-100 (Sigma Aldridge, St-Louis, MO) in PBS for 15 minutes at room temperature and subsequently washed with PBS three times shaking at room temperature. Samples were then incubated with 1:1000 DAPI (Invitrogen) and FITC-phalloidin (Invitrogen) and 1% bovine serum albumin (Sigma Aldridge, St-Louis, MO)

overnight at 4 °C. Samples were then washed three times with PBS shaking at room temperature and subsequently mounted on microscope slides using Fluoromount mounting medium (Sigma Aldridge, St-Louis, MO).

Traction Force Microscopy

In 2D traction force experiments, cells plated on polyacrylamide gels and were allowed to adhere and spread for 4-5 hours, after which, in conditions of serum starvation, media was aspirated, gels were washed with sterile PBS, and DMEM that did not contain any FBS was replaced.

In 3D traction force experiments, after cells were permitted to spread and adhere for 4-5 hours, media was aspirated, washed with sterile PBS, and a 12 mm gel was placed in the center of the 18 mm gel, and held there with forceps for 30 seconds. While still applying force with forceps on the top coverslip, serum-supplemented DMEM or no serum media was added to the well (Figure 5)

In both 2D and 3D experiments, cells were serum-starved and/or subjected to 3D cues for 24 hours before imaging.

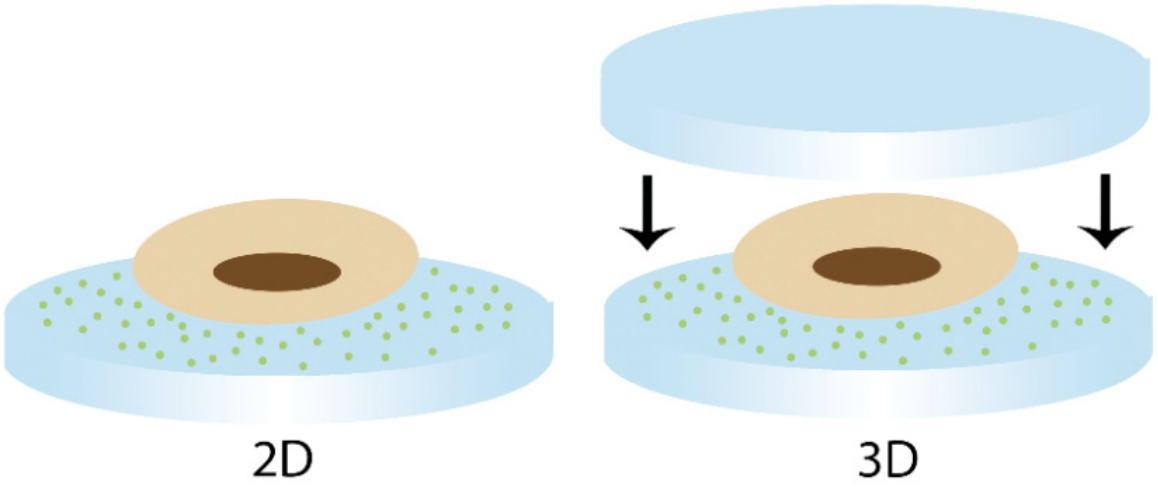

Figure 5. Schematic of traction force microscopy methodology. Traction forces were obtained from cells adhered to planar polyacrylamide gels (2D), and cells sandwiched between two gels (3D).

Imaging

Gels were placed in chamlide 18mm live magnetic imaging chamber (Live Cell Instruments, Seoul, Korea), and warm media was added to the chamber. The bottom of the coverslip was gently washed with 70% ethanol in order to prevent salt formation on the bottom coverslip. Phase contrast images of single cells adhered to the polyacrylamide were collected using using Quorum WaveFX spinning disk confocal system, on a Leica DMI6000B inverted microscope, fully motorized, with a Hamamatsu EM-CCD camera; Live Cell Instruments Chamlide TC environmental control system 10X air objective using metamorph software (Molecular Devices, SunnyVale, CA). Fluorescent confocal stress images of beads embedded

within the gel and then a killing agent, 1% (w/v) sodium dodecyl sulphate (SDS) was added and unstressed images of the beads were obtained.

Statistical Analysis

Statistical analysis was preformed using a one-way ANOVA (Newman-Keuls post-hoc test) using Prism Graphpad software (Graphad Software, La Jolla, Ca)

Results

Image processing

Template aligning, particle image velocimetry (PIV), and Fourier transform traction cytometry (FTTC) plugins on ImageJ were used to obtain traction forces from stressed and unstressed images (Tseng et al., 2012). Briefly, unstressed and stressed images were made into a stack and aligned to correct for experimental shift using the template matching software, then PIV was run to track the displacement of beads, and finally and FTTC was used to calculate and create a magnitude force map based on the displacement of the beads, pixel size the Young's Modulus of the gel, and Poisson's ration of the gel, and the maximal traction force from each cell was used (Figure 6).

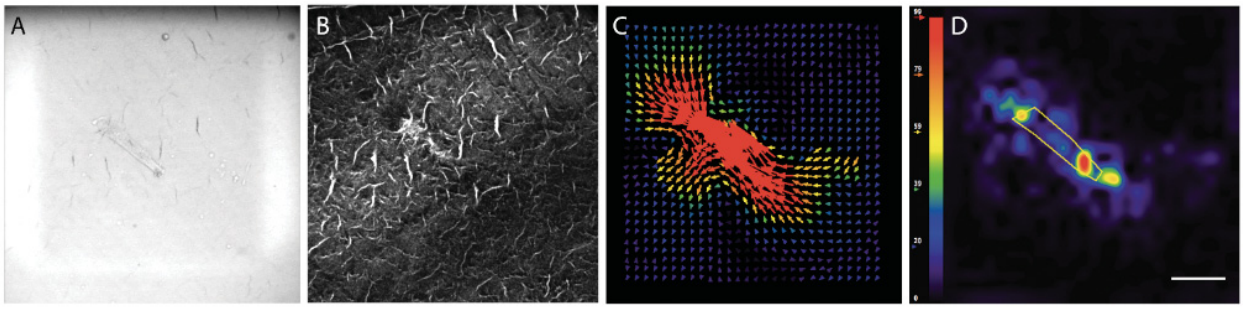

Figure 6. Traction force microscopy image analysis A) Representative image of bright field image of cell (10 X magnification). B) Representative confocal image of stressed underlying fluorescent beads (10X magnification). C) PIV was run on stressed and unstressed images to track beads displacement. D) Traction force field obtained from PIV, Young's Modulus and Poisson's ratio of the gel. Scale Bar = 80 µu.

NLF cells are sensitive to matrix stiffness and the presence of serum in 2D

In order to assess whether NLF traction forces were affected by the presence of serum and matrix stiffness, traction force microscopy was performed on NLF cells adhered to soft (E = 321 Pa) and stiff (E = 12.3 kPa) polyacrylamide gels in the presence of serum or conditions of 24 hour serum-starvation (Figure 7A). Both serum and matrix stiffness stimulates a significant increase in traction forces in NLFs on soft 2D matrices.

IPF cells respond to matrix stiffness only in absence of serum in 2D

To assess whether IPF fibroblast traction forces were affected by the presence of serum and matrix stiffness, IPF cells cells adhered to soft (E = 321 Pa) and stiff (E = 12.3 kPa) polyacrylamide gels in the presence of serum or conditions of 24 hour serum starvation (Figure 7B). IPF cell traction forces were only sensitive to the presence of serum on soft matrices, and only respond to matrix stiffness in the absence of serum.

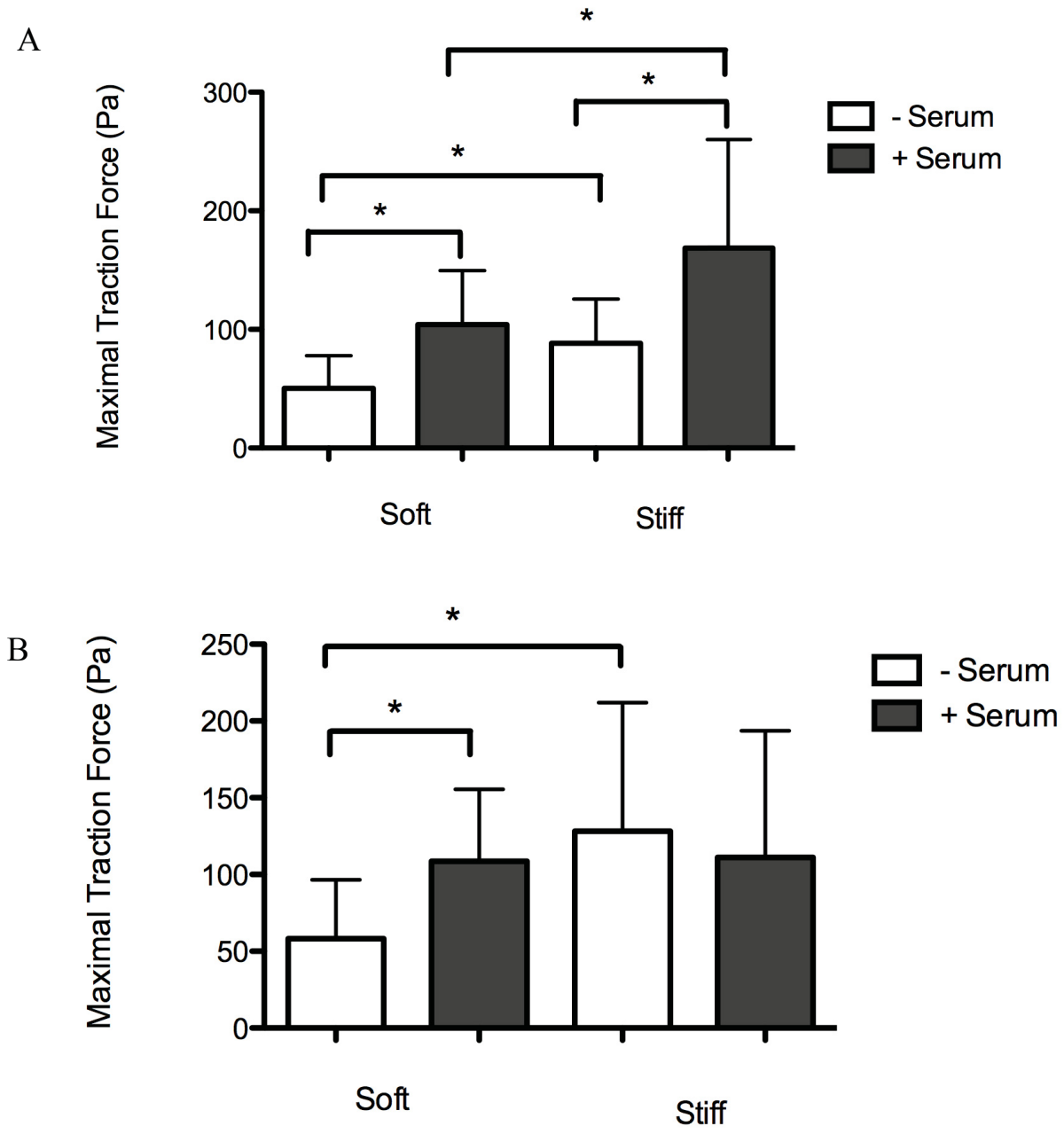

Figure 7. NLF and IPF response to matrix stiffness and serum supplementation in 2D. A) NLFs significantly increase traction forces in response to serum and increase in matrix stiffness. B) IPF cells increase traction forces in response to serum on soft matrices and increase traction forces in response to stiffness only in conditions of serum-starvation. One-way ANOVA, SNK post-test, * + P <0.05, n=20-46.

NLF and IPF traction forces in 3D are unaffected by serum on soft and stiff matrices

Considering that cells naturally interact with a 3D microenvironment, traction forces of IPF and NLF fibroblasts subjected to 3D cues in conditions of serum and serum-starvation were assessed (Figure 8). On soft (E = 321 Pa), and stiff (E = 12.3 kPa) 3D matrices (Figure 8A & 8B) similar traction forces were seen amongst both cell types in the presence and absence of serum. The results suggest that cell traction forces are unaffected by the presence of serum on soft 3D matrices in both healthy and diseased states. Comparing traction forces on soft and stiff matrices in 3D, both NLF and IPF cells increase traction forces in response to matrix stiffness in both presence and absence of serum.

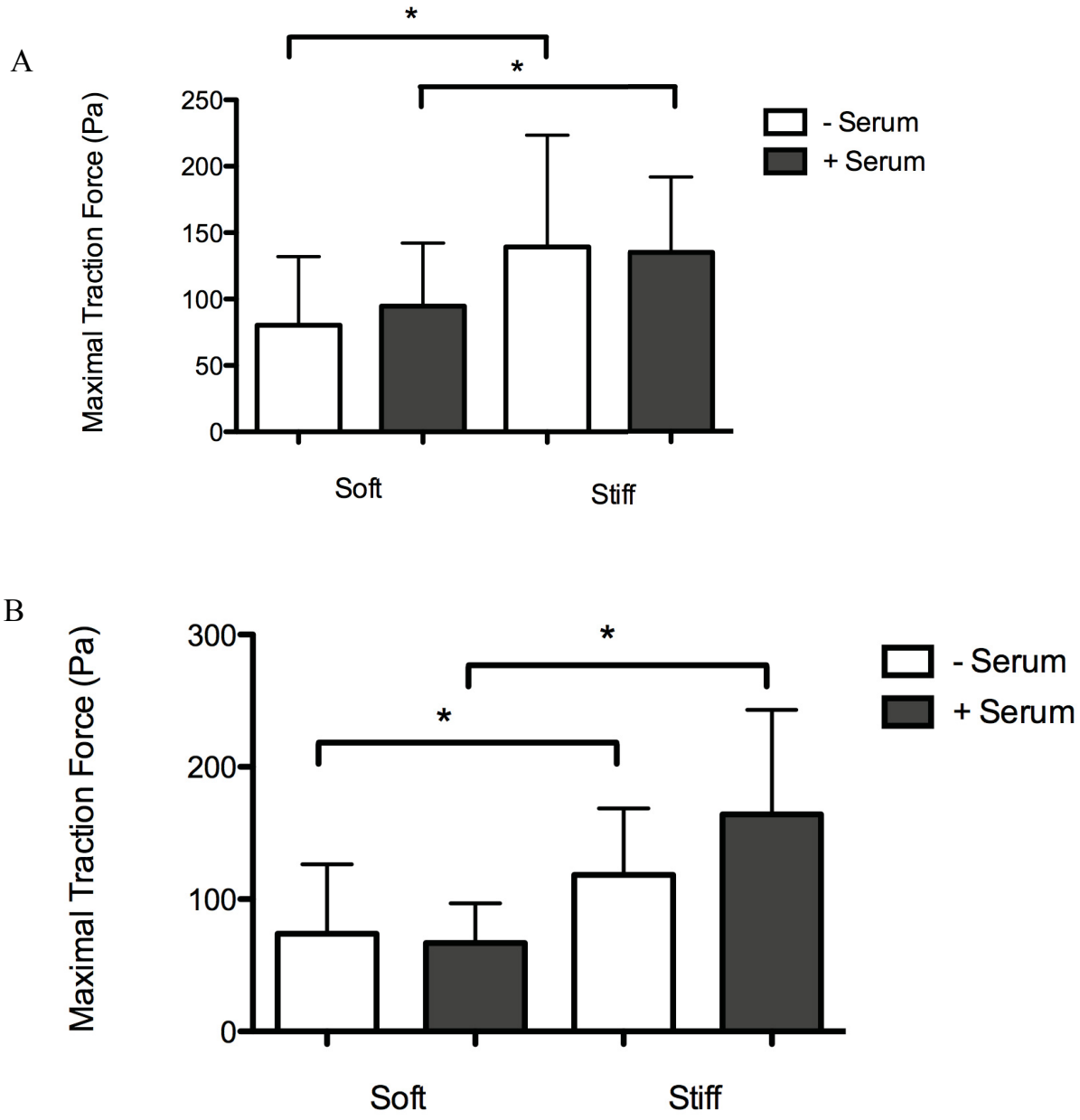

*Figure 8. NLF and IPF response to serum and matrix stiffness in 3D. A) NLF and B) IPF cells significantly increase traction forces in response to matrix stiffness in the presence and absence of serum, and are insensitive to the presence of serum. One-way ANOVA, SNK post-test, * = P<0.05, n=20-46*

NLF morphology is not affected by dimensionality

The length, width and aspect ratio of NLF cells were measured using the bright field images obtained during traction force microscopy acquisition. Cells were elongated and fibular regardless of culture condition, and there is no difference in fibroblast morphology in 2D and 3D (Figure 9) .

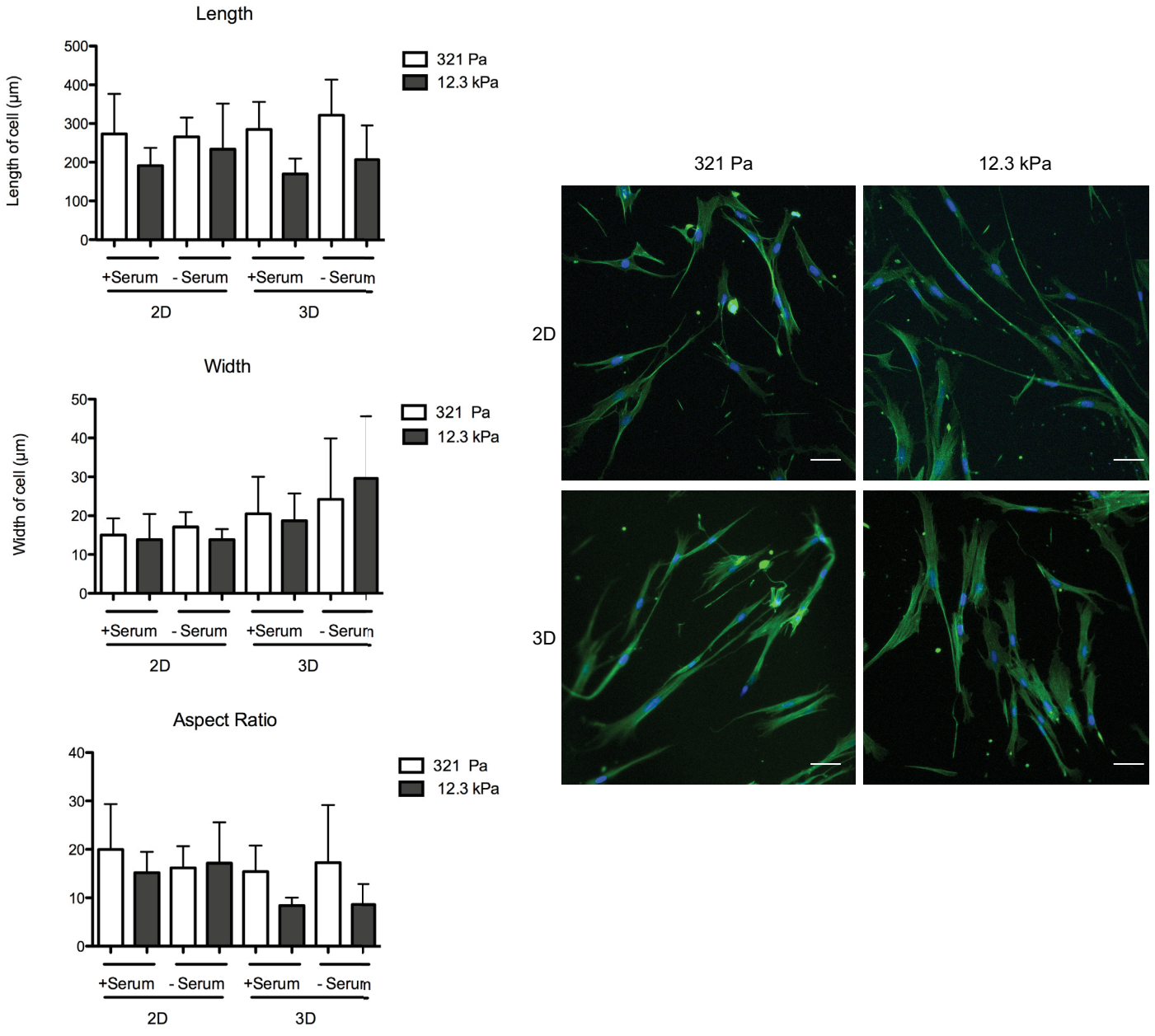

Figure 9. NLF morphology is not affected by dimensionality. A) Quantitative characterization of length, width, aspect ratio. B) Fluorescent images of NLF cells on 321 Pa and 12.3 kPa gels in 2D and 3D, scale bar = 50µm. No changes in cell morphology between 2D and 3D One-way ANOVA, SNK post-test, * + P <0.05, n=2-21.

Discussion

Idiopathic pulmonary fibrosis is the most common interstitial pneumonia of unknown cause or cure and poor prognosis of 2.5-4 years after diagnosis (Renzoni et al., 2014; Wolters et al., 2014). The main effector cell in IPF is the fibroblast, which under pathological conditions differentiates into myofibroblasts that secretes ECM and contract the matrix resulting in characteristic fibroblastic foci and increased matrix stiffness (Bochaton-Piallat et al., 2016). Current rodent models do not recapitulate many key features of this disease (Moeller et al., 2008) and a human *in vitro* drug discovery platform is needed. In this is study we sought to uncover parameters that are often ignored in conventional *in vitro* studies that may significantly affect lung fibroblast biomechanics. We hypothesize that stiffness, dimensionality and serum-supplementation of the culture system effects the biomechanical output of primary IPF and NLF fibroblast cells. Using traction force microscopy, we studied the effects of each of these parameters in isolation and in combination to understand how the biomechanical output IPF and NLF cells are affected by these factors.

FBS is the gold-standard supplement used in universally all cell culture to stimulate cell growth and proliferation, despite that its contents are largely unknown. It has long been understood that medium containing serum alters cell behaviour and phenotype. Serum activates a highly conserved transcription factor, serum response factor (SRF), that activates actin cytoskeletal organization, cellular contraction and myofibroblast differentiation (Miano, Long, & Fujiwara, 2007). Both NLF and IPF fibroblasts traction forces on 2D soft matrices (Figure 7) and collagen microgel contraction (Figure 4) respond robustly to the presence of serum. Interestingly, serum-induced contraction of fibroblasts can be attenuated by the removal of fibronectin from

the serum (Gillery et al., 1986). The ED-A domain of fibronectin is only expressed during wound healing and fibrosis and is a known stimulator of IPF (Serini et al., 1998), and this may elucidate an underlying mechanism of IPF initiation. Taken together, the previous studies and data shown here, demonstrate that serum clearly affects IPF and NLF traction force generation *in vitro*.

Both IPF and NLF traction forces subjected to 3D cues on both soft and stiff matrices, were not affected by the presence of serum (Figure 8). Cells *in vivo* routinely interact with 3D cues, and it has recently become understood that cells behave differently in 2D compared to 3D microenvironments (B. M. Baker & Chen, 2012; Harunaga & Yamada, 2011; Magin, Alge, & Anseth, 2016). In 2D cultures, cells flatten out and an apical-basal polarity is forced upon them, and this is not an issue with epithelial cells as they have inherent polarity (B. M. Baker & Chen, 2012). However, fibroblasts do not naturally have polarity, and therefore 2D culture systems stimulate an artificial compartmentalization in fibroblasts which results in differences in cell behaviour. Sandwiching fibroblasts between two compliant hydrogels has been shown to negate the artificial polarity of 2D planar systems, resulting in changes in fibroblast morphology and cell-matrix adhesions (Beningo et al., 2004). Interestingly, changes in fibroblast morphology were not observed (Figure 9), we speculate that this is due to mechanosensory differences between primary and immortalized cells, and further experimentation is underway. Fibroblast robust and differential response to serum in 2D compared to 3D, may be a result of differential cytoskeletal arrangements, adhesion sites, that have been shown to be dimensionality-dependent (Huebsch et al., 2010). Alternatively, in the 3D traction force experiments, serum may not have been able to penetrate through the two gels. This is an unlikely explanation, as the gels were incubated for 24 hours before microscopy, which would allow sufficient time for serum to

diffuse through the narrow space between the two gels. Taken together, the results demonstrate that IPF and NLF fibroblasts respond differently to the presence of serum in 2D compared to 3D.

Most notably, from the collagen microgel contraction assay (Figure 4), a significant difference between NLF and IPF contraction was seen in the absence of serum and this trend was not observed in traction force experiments in any of the conditions tested. Essentially, NLF and IPF cells are not behaving as distinct cell types in the traction force microscopy experiments, and this can be due to a number of reasons including, NLF differentiation into protomyofibroblasts, IPF cell senescence, polyacrylamide stiffness, and functional differences between the two assays.

Firstly, NLFs may have partially differentiated into protomyofibroblasts, since fibroblasts that are obtained from various connective tissues or organs and placed into plastic tissue culture dishes rapidly acquire a protomyofibroblast phenotype via expression of stress fibres, focal adhesions, and fibronectin fibrils (Tomasek et al., 2002). Alternatively, IPF fibroblast may have de-differentiated back into fibroblasts. Myofibroblast phenotype must be maintained in culture, moreover, myofibroblasts can lose their inherent characteristics via accelerated senescence and revert back to a normal fibroblast phenotype (Bochaton-Piallat et al., 2016). The primary cells used in the traction force microscopy experiments were P8-P19 and it is possible that the IPF cells senesced and lost their *in vivo* characteristics. Biochemical characterization, for example, staining for α-SMA incorporation into actin stress fibres, is required to fully understand whether the cells are truly myofibroblasts.

Alternatively, mechanical strain is the key stimulus to maintain myofibroblast phenotype in culture (Pelham & Wang et al Nat protcl 1997). It has been shown that even in the presence of both potent fibrosis stimulators TGF-β and the ED-A domain of fibronectin, mechanical strain is

necessary to maintain myofibroblast phenotype in culture (Hinz, Mastrangelo, Iselin, Chaponnier, & Gabbiani, 2001). The polyacrylamide gels were fabricated using established recipes corresponding to various Young's Moduli (Tse & Engler, 2010). However, upon rheological testing gels were substantially softer than anticipated (Figure 10). The IPF lung stiffens to 20 kPa, therefore 12 kPa stiffness used in these experiments is an intermediate stiffness in IPF disease progression, and possibly not sufficient to maintain the myofibroblast characteristic of the primary IPF cells. In 3D traction force experiments (**Error! Reference ource not found.**), both NLF and IPF increase traction forces in response to this intermediary disease stiffness, suggesting that differences between IPF and NLF traction forces may be distinguished on stiffer matrices. In a previous study, substantial differences between IPF and NLF fibroblast traction forces were only seen on matrices of 20 kPa (Marinković et al., 2013), and further experimentation with stiffer gels will be conducted.

An additional limitation to this study is that the deposition of collagen on the surface of the polyacrylamide gels has been shown to alter the mechanical properties of the system by increasing the modulus cells experience in the plane of measurement. Collagen fibrillization on the surface of the gel causes cells to sense a different mechanoenvironment from the bulk stiffness of the underlying polyacrylamide gel (Trappmann et al., 2012). This is not an issue for other ECM proteins such as fibronectin which does not fibrillize on the surface, however collagen was necessary in this experimental setup as fibronectin is a potent stimulator of IPF (Gillery et al., 1986; Serini et al., 1998) and in order to maintain the cells at a baseline quiescent state, collagen was the only choice. In future work, indentation-based measurements of the polyacrylamide gels before and after collagen deposition will be acquired in order to more accurately characterize the mechanical properties of the gels.

Furthermore, differences between the collagen microgel results and traction force data can be attributed to the inherent functional differences between the two systems. In a collagen microgel assay, cells and the collagen matrix engage in a feedback loop whereby cellular contraction and collagen remodelling causes the collagen to stiffen. In contrast, cells placed on a polyacrylamide gel functionalized with collagen do not engage in feedback with one another. While the cells can contract and remodel the gel, the gel itself does not feedback to the stimulus. In the most severe cases of IPF, pathologically activated fibroblasts and the fibrotic ECM engage in a perpetuating negative feedback loop (Liu et al., 2010). Therefore, the cross-talk between cells and surrounding matrix that is present in the microgel contraction, may play a pivotal role in IPF cell activation and contraction.

Another notable difference between collagen microgel assay and traction force experiments in general is that traction forces are done on elastic materials whereas a collagen microgel is considered a viscoelastic and degradable system (Khetan et al., 2013). Elastic properties allow for straight forward and direct calculations of traction forces based on deformations of the underlying material, however tissues in the body are naturally viscoelastic, and may be an important physical parameter that respond to (Yu & Gen, 2011). Studies analyzing and comparing traction forces on linear elastic hydrogels and viscoelastic agarose gels indicate that traction forces are indeed different, and ignoring the viscous component may have significant impact on results obtained from cellular traction forces (Toyjanova et al., 2014). IPF and NLF cells may have been responding to the viscoelastic properties of the collagen microgel, and that may have imparted differences in cell contraction behavior between the two assays. Although accounting for viscosity of the material requires complicated simulations to calculate

traction forces, it is an important consideration when designing physiologically realistic *in vitro* culture systems.

Moreover, alveoli are composed of heterogeneous cell types including, specialized alveolar epithelial cells, endothelial cells, and immune cells (Crapo, Barry, Gehr, Bachofen, & Weibel, 1982). Although fibroblasts and myofibroblasts are the key effector cells of IPF, studying their behaviour in isolation does not give a complete picture of IPF. Co-culture of normal and IPF fibroblast with lung epithelial cells have shown that in response to epithelial injury, NLF and IPF fibroblast stimulate differential wound healing response, and IPF fibroblasts stimulate mesenchymal marker expression in post-repair epithelial cells (Prasad et al., 2014). This supports that cross-talk between epithelial cells and fibroblasts play an integral role in promoting disease initiation and progression, and an important avenue to explore in future *in vivo* human models of IPF. Further co-culture experiments have shown that IPF fibroblasts contribute to chronic inflammation via interaction with dendritic cells (Freynet et al., 2016), and stimulates vascular remodelling (Smadja et al., 2014). Taken together, understanding the interaction between fibroblasts and their neighbouring cells will be integral to creating a physiologically-realistic human model of IPF.

Conclusion

In this work we sought to investigate the effects of serum, stiffness. And dimensionality on healthy and diseased human primary lung fibroblast traction force generation with the goal of understanding the parameters important for an *in vitro* human model of IPF. Based on the robust and artificial biomechanical response of NLF and IPF cells to serum in both collagen microgel contraction experiments and 2D traction force experiments, serum clearly affects IPF traction force generation *in vitro*. In addition, IPF and NLF cells increase traction forces in response to

matrix stiffness in both 2D (in absence of serum) and 3D, indicating that matrix stiffness is an important parameter regulating fibroblast traction force generation. Furthermore, cellular responses to serum are different in 2D compared to 3D, demonstrating that IPF and NLF traction forces are affected by the dimensionality of the culture system. Dimensionality, stiffness, and serum have all been shown to affect the biomechanical output of lung fibroblast, suggesting these are important parameters to consider for a future *in vitro* human IPF model.

Appendix

Appendix A – Rheology Data

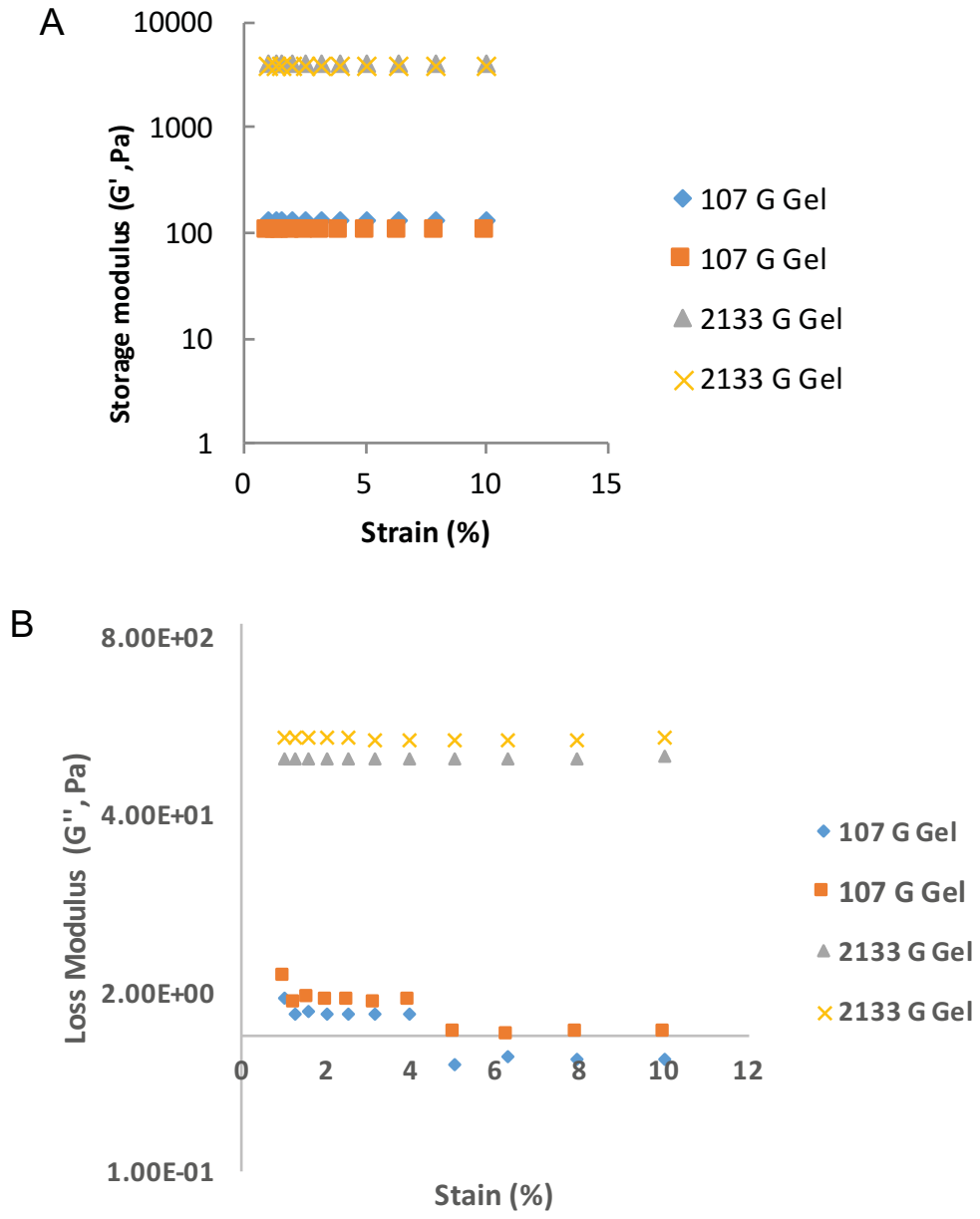

Figure 10. Characterization of polyacrylamide gels by shear rheometry A) Storage Modulus (G') and B) Loss Modulus (G''), the stiffness of the gels used was determined by shear rheometry. Two gels per stiffness were tested and the average stiffness was used in traction force calculations.

Appendix B – Development of a physiologically-realistic culture system to quantify IPF and NLF contraction

Aim: Develop a device to quantify microstissue mechanics of IPF and healthy fibroblasts in a physiologically-realistic culture environment.

Materials and Methods

Supersoft Lithography

Conventional soft lithography cannot be used to faithfully mold microfeatures in very soft polydimethylsiloxane (PDMS). A supersoft lithography method that was previously developed (Moraes et al., 2015) was used in order to mold microposts into supersoft PDMS (E= 1kPa) (Dow Corning, Auburn, MI)) (Figure 11). A silicon master mold was previously made using conventional SU-8 fabrication methods. A replica was made using hard PDMS by mixing a 10:1 (w:w) ratio of polymer to crosslinker, degassed to remove air bubblies, and cured at 70 °C for two hours. Once cured, the PDMS mold was plasma oxidized (BD-20AC, Laboratory Corona Treater) to a silicone cupcake mold and placed in an oven at 70 °C overnight to stabilize the bond. A 2:1 mixture of sugar (Redpath, Toronto, ON) to corn syrup (ACH food companies, Mississauga, ON) was made, placed in the cupcake mold that contains the hard PDMS mold and microwaved until the sugar caramelized. While the candy still hot, a pipette tip was used to remove air bubbles from the device features. Once the candy cooled, it was pealed from the cupcake PDMS mold, and henceforth served as mold for soft PDMS. Soft PDMS was mixed at 1:1 (w:w) ratio of polymer to crosslinker, and poured into the candy mold and placed in a 12-well plate. A rubber-gloved finger was used to remove air bubbles from the soft PDMS inside the device features. The device was left to cure in a desiccator containing Drierite (Drierite, Xenia, OH) for 24 hours at room temperature. Once the device cured, the device was placed in a container containing reverse osmosis (RO) water rotating until all of the candy sugar dissolved,

and then placed in a UV chamber to sterilize for 45-60 minutes. In order to visualize changes in post diameter, the device was then incubated with 1 µg/mL of DiI (Invitrogen), and washed three times for 5 minutes with sterile PBS rotating.

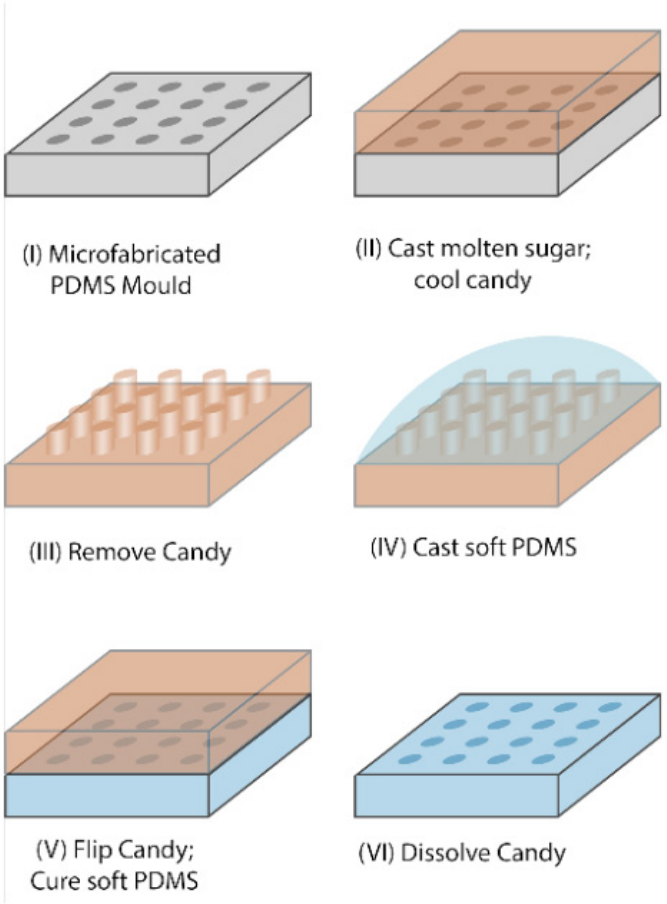

Figure 11. Schematic of sugar moulding technique. Microfeatures were patterned using a supersoft lithography method: (I) A hard PDMS master mold was used as a template for (II) molten candy. (III) Candy was removed once it hardened (IV) and used as a template for soft PDMS. Once soft PDMS was cure (V & VI) sugar was dissolved away with water and microfeatures faithfully remained in soft PDMS

Collagen Gel Formation

Bovine Collagen I gels were made using a previously described protocol (Ibidi, Fabrication of Collagen Gels). Briefly, a 1.5 mg/mL gel was made by combining, in the following order, 20 µL 10X DMEM (Sigma Aldridge, St-Louis, MO), 6 µL freshly made and filter-sterilized 1M Sodium Hydroxide (NaOH, Sigma-Aldridge, St-Louis, MO), 14 µL sterile water, 10 µL 7.5% filter-sterilized sodium bicarbonate (Sigma-Aldridge, St-Louis, MO), 50 µL 1X DMEM, 150 µL 3 mg/mL Bovine Collagen I, and 50 µL of a 6.0 X 10^6 cells/mL cell suspension. Once everything was gently and thoroughly mixed together and the solution was a pale pink color indicating a neutral pH, the unpolymerized collagen mixture was pipetted onto the soft PDMS device, the cells were allowed to settle for 5 minutes and the excess collagen was aspirated, the device was placed in a humid incubator at 5% CO_2 at 37 °C for one hour to form a gel, and media was added, and the devices were placed in 10% CO_2 incubator for 24 hours to allow for compaction of the collagen gel.

Results

Fabrication of physiologically-realistic device to measure fibroblast contraction

Considering the natural architecture of lung alveoli, whereby cells surround a hollow air sac, a soft PDMS device with a central micropost was fabricated using supersoft lithography (Figure 12). Initial attempts at creating a master mold made of candy were sabotaged due to the humidity in the lab which dissolved the microfeatures in the sugar. Humidity issues were circumvented by avoiding sugar molding on extremely humid days, and allowing PDMS to cure at room temperature for 24 hours in a desiccator rather than in an oven. IPF and NLF cells embedded within 3D collagen matrices were seeded into the device and collagen contraction around the central post was observed

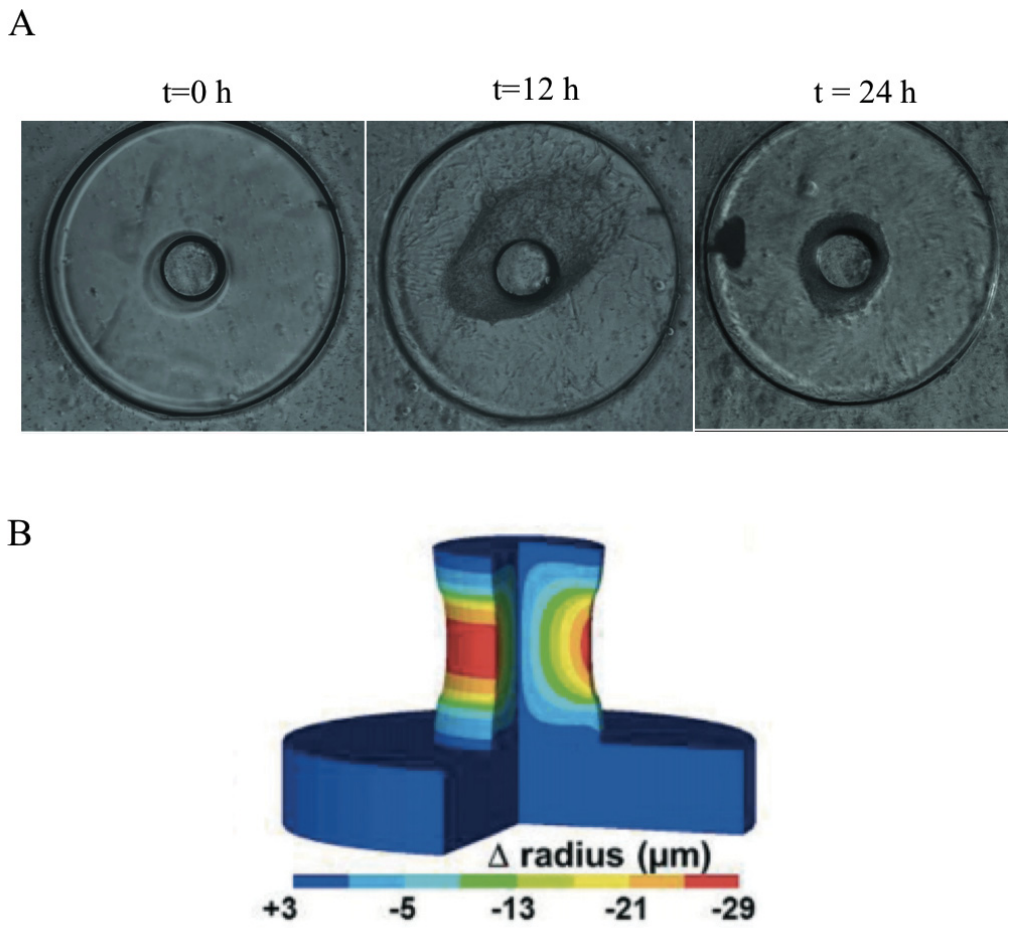

Figure 12. . Fabrication of a physiologically-realistic device to measure NLF and IPF cell contraction. A) Soft PDMS microwells containing a central micropost that mimics the alveolar architecture was successfully fabricated. Cells embedded within collagen microgels were seeded with in the device and allowed to contract for 24 hours. B) Finite element contraction of the soft micropost reused with permission from (Moraes et al., 2015)

References

Adamson, I. Y. R., & Bowden, D. H. (1974). The Pathogenesis of Bleomycin-Induced Pulmonary Fibrosis in Mice. *Am J Pathol, 77*(2), 185-198.

Ali, M. Y., Chuang, C. Y., & Saif, M. T. (2014). Reprogramming cellular phenotype by soft collagen gels. *Soft Matter, 10*(44), 8829-8837. doi:10.1039/c4sm01602e

Baker, B. M., & Chen, C. S. (2012). Deconstructing the third dimension: how 3D culture microenvironments alter cellular cues. *J Cell Sci, 125*(Pt 13), 3015-3024. doi:10.1242/jcs.079509

Baker, B. M., Trappmann, B., Wang, W. Y., Sakar, M. S., Kim, I. L., Shenoy, V. B., . . . Chen, C. S. (2015). Cell-mediated fibre recruitment drives extracellular matrix mechanosensing in engineered fibrillar microenvironments. *Nat Mater, 14*(12), 1262-1268. doi:10.1038/nmat4444

http://www.nature.com/nmat/journal/v14/n12/abs/nmat4444.html - supplementary-information

Ballester-Beltrán, J., Moratal, D., Lebourg, M., & Salmerón-Sánchez, M. (2014). Fibronectin-matrix sandwich-like microenvironments to manipulate cell fate. *Biomaterials Science, 2*(3), 381-389.

Ballester‐Beltrán, J., Lebourg, M., & Salmerón‐Sánchez, M. (2013). Dorsal and ventral stimuli in sandwich‐like microenvironments. Effect on cell differentiation. *Biotechnol Bioeng, 110*(11), 3048-3058.

Bell, E., Ivarsson, B., & Merrill, C. (1979). Production of a tissue-like structure by contraction of collagen lattices by human fibroblasts of different proliferative potential in vitro. *Proc Natl Acad Sci U S A, 76*(3), 1274-1278.

Beningo, K. A., Dembo, M., & Wang, Y. L. (2004). Responses of fibroblasts to anchorage of dorsal extracellular matrix receptors. *Proc Natl Acad Sci U S A, 101*(52), 18024-18029. doi:10.1073/pnas.0405747102

Bochaton-Piallat, M. L., Gabbiani, G., & Hinz, B. (2016). The myofibroblast in wound healing and fibrosis: answered and unanswered questions. *F1000Res, 5*. doi:10.12688/f1000research.8190.1

Bonnans, C., Chou, J., & Werb, Z. (2014). Remodelling the extracellular matrix in development and disease. *Nat Rev Mol Cell Biol, 15*(12), 786-801. doi:10.1038/nrm3904

Canestaro, W. J., Forrester, S. H., Raghu, G., Ho, L., & Devine, B. E. (2016). Drug Treatment of Idiopathic Pulmonary Fibrosis: Systematic Review and Network Meta-Analysis. *Chest, 149*(3), 756-766. doi:http://dx.doi.org/10.1016/j.chest.2015.11.013

Cen, L., Liu, W., Cui, L., Zhang, W., & Cao, Y. (2008). Collagen Tissue Engineering: Development of Novel Biomaterials and Applications. *Pediatr Res, 63*(5), 492-496.

Charras, G., & Sahai, E. (2014). Physical influences of the extracellular environment on cell migration. *Nat Rev Mol Cell Biol, 15*(12), 813-824. doi:10.1038/nrm3897

Chen, C. S., Alonso, J. L., Ostuni, E., Whitesides, G. M., & Ingber, D. E. (2003). Cell shape provides global control of focal adhesion assembly. *Biochem Biophys Res Commun, 307*(2), 355-361.

Cox, T. R., & Erler, J. T. (2011). Remodeling and homeostasis of the extracellular matrix: implications for fibrotic diseases and cancer. *Dis Model Mech, 4*(2), 165-178. doi:10.1242/dmm.004077

Crapo, J. D., Barry, B. E., Gehr, P., Bachofen, M., & Weibel, E. R. (1982). Cell number and cell characteristics of the normal human lung. *Am Rev Respir Dis, 126*(2), 332-337. doi:10.1164/arrd.1982.126.2.332

Daccord, C., & Maher, T. M. (2016). Recent advances in understanding idiopathic pulmonary fibrosis. *F1000Res, 5*. doi:10.12688/f1000research.8209.1

Dembo, M., & Wang, Y. L. (1999). Stresses at the cell-to-substrate interface during locomotion of fibroblasts. *Biophysical Journal, 76*(4), 2307-2316.

DiMasi, J. A., Grabowski, H. G., & Hansen, R. W. (2016). Innovation in the pharmaceutical industry: New estimates of R&D costs. *J Health Econ, 47*, 20-33. doi:10.1016/j.jhealeco.2016.01.012

Dupont, S., Morsut, L., Aragona, M., Enzo, E., Giulitti, S., Cordenonsi, M., . . . Piccolo, S. (2011). Role of YAP/TAZ in mechanotransduction. *Nature, 474*(7350), 179-183. doi:http://www.nature.com/nature/journal/v474/n7350/abs/10.1038-nature10137-unlocked.html - supplementary-information

Engler, A. J., Sen, S., Sweeney, H. L., & Discher, D. E. (2006). Matrix elasticity directs stem cell lineage specification. *Cell, 126*(4), 677-689. doi:10.1016/j.cell.2006.06.044

Felder, M., Stucki, A. O., Stucki, J. D., Geiser, T., & Guenat, O. T. (2014). The potential of microfluidic lung epithelial wounding: towards in vivo-like alveolar microinjuries. *Integr Biol (Camb), 6*(12), 1132-1140. doi:10.1039/c4ib00149d

Freynet, O., Marchal-Somme, J., Jean-Louis, F., Mailleux, A., Crestani, B., Soler, P., & Michel, L. (2016). Human lung fibroblasts may modulate dendritic cell phenotype and function: results from a pilot in vitro study. *Respir Res, 17*, 36. doi:10.1186/s12931-016-0345-4

Gabbiani, G., Le Lous, M., Bailey, A. J., Bazin, S., & Delaunay, A. (1976). Collagen and myofibroblasts of granulation tissue. *Virchows Archiv B, 21*(1), 133-145. doi:10.1007/BF02899150

Gillery, P., Maquart, F. X., & Borel, J. P. (1986). Fibronectin dependence of the contraction of collagen lattices by human skin fibroblasts. *Experimental cell research, 167*(1), 29-37. doi:10.1016/0014-4827(86)90201-6

Hakkinen, K. M., Harunaga, J. S., Doyle, A. D., & Yamada, K. M. (2011). Direct Comparisons of the Morphology, Migration, Cell Adhesions, and Actin Cytoskeleton of Fibroblasts in Four Different Three-Dimensional Extracellular Matrices. *Tissue Eng Part A, 17*(5-6), 713-724. doi:10.1089/ten.tea.2010.0273

Harunaga, J. S., & Yamada, K. M. (2011). Cell-matrix adhesions in 3D. *Matrix Biol, 30*(7-8), 363-368. doi:10.1016/j.matbio.2011.06.001

Hinz, B., Mastrangelo, D., Iselin, C. E., Chaponnier, C., & Gabbiani, G. (2001). Mechanical tension controls granulation tissue contractile activity and myofibroblast differentiation. *Am J Pathol, 159*(3), 1009-1020. doi:10.1016/s0002-9440(10)61776-2

Hinz, B., Phan, S. H., Thannickal, V. J., Galli, A., Bochaton-Piallat, M. L., & Gabbiani, G. (2007). The myofibroblast: one function, multiple origins. *Am J Pathol, 170*(6), 1807-1816. doi:10.2353/ajpath.2007.070112

Hoon, L. J., Tan, H. M., & Koh, C.-G. (2016). The Regulation of Cellular Responses to Mechanical Cues by Rho GTPases. *Cells, 5*(2). doi:10.3390/cells5020017

Huang, S. K., & Horowitz, J. C. (2014). Outstaying their Welcome: The Persistent Myofibroblast in IPF. *Austin journal of pulmonary and respiratory medicine, 1*(1), 3.

Huang, X., Yang, N., Fiore, V. F., Barker, T. H., Sun, Y., Morris, S. W., . . . Zhou, Y. (2012). Matrix stiffness-induced myofibroblast differentiation is mediated by intrinsic mechanotransduction. *Am J Respir Cell Mol Biol, 47*(3), 340-348. doi:10.1165/rcmb.2012-0050OC

Huebsch, N., Arany, P. R., Mao, A. S., Shvartsman, D., Ali, O. A., Bencherif, S. A., . . . Mooney, D. J. (2010). Harnessing traction-mediated manipulation of the cell/matrix interface to control stem-cell fate. *Nat Mater, 9*(6), 518-526. doi:http://www.nature.com/nmat/journal/v9/n6/suppinfo/nmat2732_S1.html

Humphrey, J. D., Dufresne, E. R., & Schwartz, M. A. (2014). Mechanotransduction and extracellular matrix homeostasis. *Nat Rev Mol Cell Biol, 15*(12), 802-812. doi:10.1038/nrm3896

Ingber, D. E. (2016). Reverse Engineering Human Pathophysiology with Organs-on-Chips. *Cell, 164*(6), 1105-1109. doi:10.1016/j.cell.2016.02.049

Irianto, J., Pfeifer, C. R., Xia, Y., & Discher, D. E. (2016). SnapShot: Mechanosensing Matrix. *Cell, 165*(7), 1820-1820.e1821. doi:http://dx.doi.org/10.1016/j.cell.2016.06.002

Izbicki, G., Segel, M. J., Christensen, T. G., Conner, M. W., & Breuer, R. (2002). Time course of bleomycin-induced lung fibrosis. *Int J Exp Pathol, 83*(3), 111-119.

Joaquin, D., Grigola, M., Kwon, G., Blasius, C., Han, Y., Perlitz, D., . . . Hsia, K. J. (2016). Cell migration and organization in three-dimensional in vitro culture driven by stiffness gradient. *Biotechnol Bioeng*. doi:10.1002/bit.26010

Kanta, J. (2015). Collagen matrix as a tool in studying fibroblastic cell behavior. *Cell Adh Migr, 9*(4), 308-316. doi:10.1080/19336918.2015.1005469

Khetan, S., Guvendiren, M., Legant, W. R., Cohen, D. M., Chen, C. S., & Burdick, J. A. (2013). Degradation-mediated cellular traction directs stem cell fate in covalently crosslinked three-dimensional hydrogels. *Nat Mater, 12*(5), 458-465. doi:10.1038/nmat3586

Kim, D. S., Collard, H. R., & King, T. E. (2006). Classification and Natural History of the Idiopathic Interstitial Pneumonias. *Proceedings of the American Thoracic Society, 3*(4), 285-292. doi:10.1513/pats.200601-005TK

Kim, K. K., Kugler, M. C., Wolters, P. J., Robillard, L., Galvez, M. G., Brumwell, A. N., . . . Chapman, H. A. (2006). Alveolar epithelial cell mesenchymal transition develops in vivo during pulmonary fibrosis and is regulated by the extracellular matrix. *Proc Natl Acad Sci U S A, 103*(35), 13180-13185. doi:10.1073/pnas.0605669103

Klingberg, F., Hinz, B., & White, E. S. (2013). The myofibroblast matrix: implications for tissue repair and fibrosis. *J Pathol, 229*(2), 298-309. doi:10.1002/path.4104

Kojima, T., Moraes, C., Cavnar, S. P., Luker, G. D., & Takayama, S. (2015). Surface-templated hydrogel patterns prompt matrix-dependent migration of breast cancer cells towards chemokine-secreting cells. *Acta Biomater, 13*, 68-77. doi:10.1016/j.actbio.2014.11.033

Kraning-Rush, C. M., Califano, J. P., & Reinhart-King, C. A. (2012). Cellular Traction Stresses Increase with Increasing Metastatic Potential. *PLoS ONE, 7*(2), e32572. doi:10.1371/journal.pone.0032572

Lee, J. S., Collard, H. R., Raghu, G., Sweet, M. P., Hays, S. R., Campos, G. M., . . . King, T. E. (2010). Does Chronic Microaspiration Cause Idiopathic Pulmonary Fibrosis? *The American journal of medicine, 123*(4), 304-311. doi:10.1016/j.amjmed.2009.07.033

Legant, W. R., Miller, J. S., Blakely, B. L., Cohen, D. M., Genin, G. M., & Chen, C. S. (2010). Measurement of mechanical tractions exerted by cells in three-dimensional matrices. *Nat Meth, 7*(12), 969-971. doi:http://www.nature.com/nmeth/journal/v7/n12/abs/nmeth.1531.html - supplementary-information

Legant, W. R., Miller, J. S., Blakely, B. L., Cohen, D. M., Genin, G. M., & Chen, C. S. (2010). Measurement of mechanical tractions exerted by cells within three-dimensional matrices. *Nat Methods, 7*(12), 969-971. doi:10.1038/nmeth.1531

Leung, B. M., Moraes, C., Cavnar, S. P., Luker, K. E., Luker, G. D., & Takayama, S. (2015). Microscale 3D collagen cell culture assays in conventional flat-bottom 384-well plates. *J Lab Autom, 20*(2), 138-145. doi:10.1177/2211068214563793

Li, B., & Wang, J. H. (2011). Fibroblasts and myofibroblasts in wound healing: force generation and measurement. *J Tissue Viability, 20*(4), 108-120. doi:10.1016/j.jtv.2009.11.004

Li, Y., & Kilian, K. A. (2015). Bridging the Gap: From 2D Cell Culture to 3D Microengineered Extracellular Matrices. *Adv Healthc Mater, 4*(18), 2780-2796. doi:10.1002/adhm.201500427

Liu, F., Mih, J. D., Shea, B. S., Kho, A. T., Sharif, A. S., Tager, A. M., & Tschumperlin, D. J. (2010). Feedback amplification of fibrosis through matrix stiffening and COX-2 suppression. *J Cell Biol, 190*(4), 693-706. doi:10.1083/jcb.201004082

Magin, C. M., Alge, D. L., & Anseth, K. S. (2016). Bio-inspired 3D microenvironments: a new dimension in tissue engineering. *Biomed Mater, 11*(2), 022001. doi:10.1088/1748-6041/11/2/022001

Marinković, A., Liu, F., & Tschumperlin, D. J. (2013). Matrices of Physiologic Stiffness Potently Inactivate Idiopathic Pulmonary Fibrosis Fibroblasts. *Am J Respir Cell Mol Biol, 48*(4), 422-430. doi:10.1165/rcmb.2012-0335OC

Miano, J. M., Long, X., & Fujiwara, K. (2007). Serum response factor: master regulator of the actin cytoskeleton and contractile apparatus. *American Journal of Physiology - Cell Physiology, 292*(1), C70-C81. doi:10.1152/ajpcell.00386.2006

Moeller, A., Ask, K., Warburton, D., Gauldie, J., & Kolb, M. (2008). The bleomycin animal model: a useful tool to investigate treatment options for idiopathic pulmonary fibrosis? *The international journal of biochemistry & cell biology, 40*(3), 362-382. doi:10.1016/j.biocel.2007.08.011

Moraes, C., Labuz, J. M., Shao, Y., Fu, J., & Takayama, S. (2015). Supersoft lithography: candy-based fabrication of soft silicone microstructures. *Lab Chip, 15*(18), 3760-3765. doi:10.1039/c5lc00722d

Moraes, C., Simon, A. B., Putnam, A. J., & Takayama, S. (2013). Aqueous two-phase printing of cell-containing contractile collagen microgels. *Biomaterials, 34*(37), 9623-9631. doi:10.1016/j.biomaterials.2013.08.046

Murphy, W. L., McDevitt, T. C., & Engler, A. J. (2014). Materials as stem cell regulators. *Nat Mater, 13*(6), 547-557. doi:10.1038/nmat3937

Noble, P. W., Barkauskas, C. E., & Jiang, D. (2012). Pulmonary fibrosis: patterns and perpetrators. *The Journal of Clinical Investigation, 122*(8), 2756-2762. doi:10.1172/JCI60323

Peyton, S. R., & Putnam, A. J. (2005). Extracellular matrix rigidity governs smooth muscle cell motility in a biphasic fashion. *J Cell Physiol, 204*(1), 198-209. doi:10.1002/jcp.20274

Prasad, S., Hogaboam, C. M., & Jarai, G. (2014). Deficient repair response of IPF fibroblasts in a co-culture model of epithelial injury and repair. *Fibrogenesis Tissue Repair, 7*, 7. doi:10.1186/1755-1536-7-7

Raghu, G., Johnson, W. C., Lockhart, D., & Mageto, Y. (1999). Treatment of idiopathic pulmonary fibrosis with a new antifibrotic agent, pirfenidone: results of a prospective, open-label Phase II study. *Am J Respir Crit Care Med, 159*(4 Pt 1), 1061-1069. doi:10.1164/ajrccm.159.4.9805017

Raghu, G., Weycker, D., Edelsberg, J., Bradford, W. Z., & Oster, G. (2006). Incidence and prevalence of idiopathic pulmonary fibrosis. *Am J Respir Crit Care Med, 174*(7), 810-816. doi:10.1164/rccm.200602-163OC

Rangarajan, S., Locy, M. L., Luckhardt, T. R., & Thannickal, V. J. (2016). Targeted Therapy for Idiopathic Pulmonary Fibrosis: Where To Now? *Drugs, 76*(3), 291-300. doi:10.1007/s40265-015-0523-6

Rape, A. D., Guo, W. H., & Wang, Y. L. (2011). The regulation of traction force in relation to cell shape and focal adhesions. *Biomaterials, 32*(8), 2043-2051. doi:10.1016/j.biomaterials.2010.11.044

Reinert, T., #xe1, Baldotto, C. S. d. R., Nunes, F. A. P., & Scheliga, A. A. d. S. (2013). Bleomycin-Induced Lung Injury. *Journal of Cancer Research, 2013*, 9. doi:10.1155/2013/480608

Renzoni, E., Srihari, V., & Sestini, P. (2014). Pathogenesis of idiopathic pulmonary fibrosis: review of recent findings. *F1000Prime Rep, 6*, 69. doi:10.12703/p6-69

Rhee, S. (2009). Fibroblasts in three dimensional matrices: cell migration and matrix remodeling. *Experimental & Molecular Medicine, 41*(12), 858-865. doi:10.3858/emm.2009.41.12.096

Roberts, A. B., Sporn, M. B., Assoian, R. K., Smith, J. M., Roche, N. S., Wakefield, L. M., . . . et al. (1986). Transforming growth factor type beta: rapid induction of fibrosis and angiogenesis in vivo and stimulation of collagen formation in vitro. *Proc Natl Acad Sci U S A, 83*(12), 4167-4171.

Selman, M., King, T. E., & Pardo, A. (2001). Idiopathic pulmonary fibrosis: prevailing and evolving hypotheses about its pathogenesis and implications for therapy. *Ann Intern Med, 134*(2), 136-151.

Serini, G., Bochaton-Piallat, M. L., Ropraz, P., Geinoz, A., Borsi, L., Zardi, L., & Gabbiani, G. (1998). The fibronectin domain ED-A is crucial for myofibroblastic phenotype induction by transforming growth factor-beta1. *J Cell Biol, 142*(3), 873-881.

Smadja, D. M., Dorfmuller, P., Guerin, C. L., Bieche, I., Badoual, C., Boscolo, E., . . . Israel-Biet, D. (2014). Cooperation between human fibrocytes and endothelial colony-forming cells increases

angiogenesis via the CXCR4 pathway. *Thromb Haemost, 112*(5), 1002-1013. doi:10.1160/th13-08-0711

Small, E. M. (2012). The actin-MRTF-SRF gene regulatory axis and myofibroblast differentiation. *J Cardiovasc Transl Res, 5*(6), 794-804. doi:10.1007/s12265-012-9397-0

Stroka, K. M., Jiang, H., Chen, S. H., Tong, Z., Wirtz, D., Sun, S. X., & Konstantopoulos, K. (2014). Water permeation drives tumor cell migration in confined microenvironments. *Cell, 157*(3), 611-623. doi:10.1016/j.cell.2014.02.052

Style, R. W., Boltyanskiy, R., German, G. K., Hyland, C., MacMinn, C. W., Mertz, A. F., . . . Dufresne, E. R. (2014). Traction force microscopy in physics and biology. *Soft Matter, 10*(23), 4047-4055. doi:10.1039/C4SM00264D

Tobin, R. W., Pope, C. E., Pellegrini, C. A., Emond, M. J., Sillery, J. I. M., & Raghu, G. (1998). Increased Prevalence of Gastroesophageal Reflux in Patients with Idiopathic Pulmonary Fibrosis. *Am J Respir Crit Care Med, 158*(6), 1804-1808. doi:10.1164/ajrccm.158.6.9804105

Tomasek, J. J., Gabbiani, G., Hinz, B., Chaponnier, C., & Brown, R. A. (2002). Myofibroblasts and mechano-regulation of connective tissue remodelling. *Nat Rev Mol Cell Biol, 3*(5), 349-363. doi:10.1038/nrm809

Tomasek, J. J., Vaughan, M. B., Kropp, B. P., Gabbiani, G., Martin, M. D., Haaksma, C. J., & Hinz, B. (2006). Contraction of myofibroblasts in granulation tissue is dependent on Rho/Rho kinase/myosin light chain phosphatase activity. *Wound Repair Regen, 14*(3), 313-320. doi:10.1111/j.1743-6109.2006.00126.x

Toyjanova, J., Hannen, E., Bar-Kochba, E., Darling, E. M., Henann, D. L., & Franck, C. (2014). 3D Viscoelastic Traction Force Microscopy. *Soft Matter, 10*(40), 8095-8106. doi:10.1039/c4sm01271b

Trappmann, B., Gautrot, J. E., Connelly, J. T., Strange, D. G. T., Li, Y., Oyen, M. L., . . . Huck, W. T. S. (2012). Extracellular-matrix tethering regulates stem-cell fate. *Nat Mater, 11*(7), 642-649. doi:http://www.nature.com/nmat/journal/v11/n7/abs/nmat3339.html - supplementary-information

Tse, J. R., & Engler, A. J. (2010). Preparation of hydrogel substrates with tunable mechanical properties. *Curr Protoc Cell Biol, Chapter 10*, Unit 10.16. doi:10.1002/0471143030.cb1016s47

Tseng, Q., Duchemin-Pelletier, E., Deshiere, A., Balland, M., Guillou, H., Filhol, O., & Théry, M. (2012). Spatial organization of the extracellular matrix regulates cell–cell junction positioning. *Proceedings of the National Academy of Sciences, 109*(5), 1506-1511.

Vedula, S. R. K., Peyret, G., Cheddadi, I., Chen, T., Brugués, A., Hirata, H., . . . Ladoux, B. (2015). Mechanics of epithelial closure over non-adherent environments. *Nat Commun, 6*. doi:10.1038/ncomms7111

Vincent, L. G., Choi, Y. S., Alonso-Latorre, B., del Alamo, J. C., & Engler, A. J. (2013). Mesenchymal stem cell durotaxis depends on substrate stiffness gradient strength. *Biotechnol J, 8*(4), 472-484. doi:10.1002/biot.201200205

Wipff, P. J., Rifkin, D. B., Meister, J. J., & Hinz, B. (2007). Myofibroblast contraction activates latent TGF-beta1 from the extracellular matrix. *J Cell Biol, 179*(6), 1311-1323. doi:10.1083/jcb.200704042

Wollin, L., Wex, E., Pautsch, A., Schnapp, G., Hostettler, K. E., Stowasser, S., & Kolb, M. (2015). Mode of action of nintedanib in the treatment of idiopathic pulmonary fibrosis. *The European Respiratory Journal, 45*(5), 1434-1445. doi:10.1183/09031936.00174914

Wolters, P. J., Collard, H. R., & Jones, K. D. (2014). Pathogenesis of idiopathic pulmonary fibrosis. *Annu Rev Pathol, 9*, 157-179. doi:10.1146/annurev-pathol-012513-104706

Wright, J. L., Cosio, M., & Churg, A. (2008). Animal models of chronic obstructive pulmonary disease. *American Journal of Physiology - Lung Cellular and Molecular Physiology, 295*(1), L1-L15. doi:10.1152/ajplung.90200.2008

Xu, J., Cong, M., Park, T. J., Scholten, D., Brenner, D. A., & Kisseleva, T. (2015). Contribution of bone marrow-derived fibrocytes to liver fibrosis. *Hepatobiliary Surgery and Nutrition, 4*(1), 34-47. doi:10.3978/j.issn.2304-3881.2015.01.01

Yeung, T., Georges, P. C., Flanagan, L. A., Marg, B., Ortiz, M., Funaki, M., . . . Janmey, P. A. (2005). Effects of substrate stiffness on cell morphology, cytoskeletal structure, and adhesion. *Cell Motil Cytoskeleton, 60*(1), 24-34. doi:10.1002/cm.20041

Young, I. H., & Bye, P. T. (2011). Gas exchange in disease: asthma, chronic obstructive pulmonary disease, cystic fibrosis, and interstitial lung disease. *Compr Physiol, 1*(2), 663-697. doi:10.1002/cphy.c090012

Yu, J., & Gen, N. (2011). Viscoelastic properties of soft tissues in a living body measured by MR elastography. *Journal of Physics: Conference Series, 290*(1), 012006.

Zhao, J., Shi, W., Wang, Y. L., Chen, H., Bringas, P., Jr., Datto, M. B., . . . Warburton, D. (2002). Smad3 deficiency attenuates bleomycin-induced pulmonary fibrosis in mice. *Am J Physiol Lung Cell Mol Physiol, 282*(3), L585-593. doi:10.1152/ajplung.00151.2001